PHILOSOPHICAL TRANSACTIONS OF THE ROYAL SOCIETY A

Phil. Trans. R. Soc. A (2012) **370**, 246–277
doi:10.1098/rsta.2011.0249

Heaving buoys, point absorbers and arrays

By Johannes Falnes[1,2,*] and Jørgen Hals[2]

[1]*Department of Physics, and* [2]*Centre for Ships and Ocean Structures (CeSOS), Norwegian University of Science and Technology (NTNU), 7491 Trondheim, Norway*

Absorption of wave energy may be considered as a phenomenon of interference between incident and radiated waves generated by an oscillating object; a wave-energy converter (WEC) that displaces water. If a WEC is very small in comparison with one wavelength, it is classified as a point absorber (PA); otherwise, as a 'quasi-point absorber'. The latter may be a dipole-mode radiator, for instance an immersed body oscillating in the surge mode or pitch mode, while a PA is so small that it should preferably be a source-mode radiator, for instance a heaving semi-submerged buoy. The power take-off capacity, the WEC's maximum swept volume and preferably also its full physical volume should be reasonably matched to the wave climate. To discuss this matter, two different upper bounds for absorbed power are applied in a 'Budal diagram'. It appears that, for a single WEC unit, a power capacity of only about 0.3 MW matches well to a typical offshore wave climate, and the full physical volume has, unfortunately, to be significantly larger than the swept volume, unless phase control is used. An example of a phase-controlled PA is presented. For a sizeable wave-power plant, an array consisting of hundreds, or even thousands, of mass-produced WEC units is required.

Keywords: wave absorption and generation; upper bounds for absorbed wave power; Budal diagram; matching power take-off capacity to wave resource; quasi-point absorbers

1. Introduction

Wave-energy research and development was stimulated by the oil crisis in 1973. In the UK, large-sized wave-energy converters (WECs), with linear horizontal extent of at least one wavelength, were extensively investigated until 1982, while in some other countries, Japan, Norway, Sweden and the USA, heaving-buoy WECs, of extent significantly smaller than a wavelength were studied [1–6]. As these buoys are floating bodies, they are source-type wave radiators when oscillating in heave mode. Other examples of source-type radiators are oscillating-water columns (OWCs) and volume-pulsating submerged bodies.

Early results of linear theory analysis showed how the principle of impedance matching also applies to optimum wave energy absorption, and that, for a single WEC unit, optimum phase may be obtained if it is in resonance with the wave (see reviews by Evans [7] and Falnes [8]). Then the unit's oscillating velocity is

*Author for correspondence (johannes.falnes@ntnu.no).

One contribution of 18 to a Theo Murphy Meeting Issue 'The peaks and troughs of wave energy: the dreams and the reality'.

in phase with the wave-excitation force. For a reasonably sized WEC unit, the resonance frequency band does not, unfortunately, coincide with the spectrum of prevailing ocean waves, and, moreover, it is disappointingly narrow. Proper phase control of the WEC oscillation may mitigate this misfit. It was already established in the 1970s that wave energy absorbers may strongly benefit from active control of the converter motion [9–14]. Moreover, also because ocean-wave heights may vary very much from one individual wave to the next one, it is very important that WECs are equipped with means for amplitude control, for which an example is considered below in §2.

In the mid-1970s, Budal and Salter independently proposed a continuous-time control method, so-called reactive control, where the power take-off (PTO) machinery needs to reverse power flow during parts of the oscillation cycle. In contrast to continuous-time control, a discrete-instant control method, where some parts or components of the system may be switched on or off at certain instants, was proposed independently by Falnes & Budal [15], Guenther *et al.* [16] and French [17]. This discrete-instant control method, which has become to be known as 'latching control' [18], is, in contrast to the continuous-time reactive-control method, a somewhat suboptimal method, with the opportunity to achieve close to perfect phase alignment without reversing the power flow through the PTO machinery. Other variants of discrete-instant control have also been proposed, such as 'unlatching control' [19] or 'declutching control' [20,21], by which the PTO of the WEC is alternately switched on and off.

In practice, the control strategy also needs to take various constraints and losses into account. Recent progress includes the application of model-predictive control to wave energy conversion [22–25]. It gives the opportunity to take both amplitude constraints and losses into account in an optimal way. A common feature of many of the control strategies that are suggested for wave energy conversion is that they require prediction of the future excitation from real sea waves. Such an online prediction was partially successful in an early latching-control experiment carried out by Budal *et al.* [26]. After more recent development, it now seems that wave prediction may be obtained with sufficient accuracy even with only local monitoring (close to the device) of the wave pressure or wave elevation [27]. Thus, for conversion of wave power, the challenge is to develop a device that exploits the invested structure and equipment at maximum, and a PTO machinery that wastes as little power as possible once it has been absorbed from the sea.

Based on the wave-interference principle that 'to absorb a wave means to generate a wave', we analyse, in §3, the optimum problem of maximizing the amount of energy that is possible to remove from an incident plane wave. Quite often, results have, traditionally, been expressed by quantities as 'absorption width' and 'capture width', which have dimension length (SI unit metre), or by dimensionless quantities, such as 'capture width ratio' and '(hydrodynamic) efficiency'. We consider it to be very unfortunate that 'efficiency' is applied to a quantity that may, in some cases, be larger than 1. Moreover, it is also misleading to refer to an 'efficiency' that may be less than 1 for cases where no energy is being dissipated into heat! Could the frequent use of these terms be partially responsible for the situation that, after decades of research, wave-energy technology is still only a 'dream', and not 'reality' yet? We should be aware that our language influences our thinking! These technical terms focus on one horizontal dimension

(in the direction of the incident wavefront). However, a WEC has two horizontal dimensions, in addition to a vertical one. A most important and urgent challenge is to develop a feasible single unit of a WEC, a unit that maximizes the power output, not with respect to the free wave power that is available in the ocean, but with respect to parameters related more directly to the WEC itself (size, cost of investment and maintenance, etc.). In §§4–6, we discuss, for simplicity, only one such parameter: the volume. In spite of this parameter deficiency, we consider absorbed power per volume to be a more relevant relation than absorbed power per wave-energy resource.

We argue, in §5, that each source-type WEC unit's power capacity should not exceed a few hundred kilowatts. Hence, a reasonably sized wave-power plant should consist of an array of many (hundreds, or even thousands) mass-produced WEC units. In a WEC system consisting of a group of power buoys, the individual units interact with each other. This may lead to some favourable or unfavourable interference, depending on the distances between units relative to the wavelength. Because of hydrodynamic interaction, the optimum oscillation phases for maximum wave power conversion are not necessarily obtained at resonance, as is the case for an isolated single power buoy.

When choosing oscillating systems for primary conversion of wave energy, it is fruitful to be aware of the fact that, in order for a WEC system to be a good wave absorber, it has to be a good wave generator. This principle is the subject of §3 below, and it is applied, firstly, when we in §§4 and 5 introduce and apply a useful tool, the 'Budal diagram', and, secondly, when source-type and dipole-type oscillation modes for an immersed body are comparatively discussed in §6.

2. An example of a heaving buoy wave-energy converter unit

For wave-energy utilization, the stochastic nature of real sea waves is a great challenge. There is a serious variation in wave periods and an even more serious variation in wave heights. It would have been much easier if the wave had always been sinusoidal with invariable amplitude and period! Then the PTO loading could have been constant and, with a proper buoy-hull size, resonance and hence optimum phase could have been always achieved. And, moreover, the required hull size could have been fully used if the wave amplitude had been sufficiently large to match this hull size. Prevailing ocean waves have heights in the region of 0.5–3 m and periods in the region of 6–10 s. For a hull size that matches these wave heights, the natural period for heave resonance is shorter than the prevailing wave periods, and, moreover, the resonance bandwidth is much too narrow to include prevailing wave frequencies.

Based on these observations, Budal [28] proposed an invention as indicated in figure 1, a heaving buoy WEC unit, which includes hydraulic components for PTO, for amplitude and phase control, and for short-time energy storage. The hull size is chosen sufficiently small to ensure that the buoy's full heave stroke is used a substantial fraction of the year. The unit is moored through a mooring cable MC (or, alternatively, a mooring strut), which is pre-tensioned by means of the pressure inside gas accumulator A1. Discrete-instant phase control is obtained by closing the operable valve V1 at instants when the heave velocity is zero, and by opening the same valve about one-quarter of a natural heave period before the

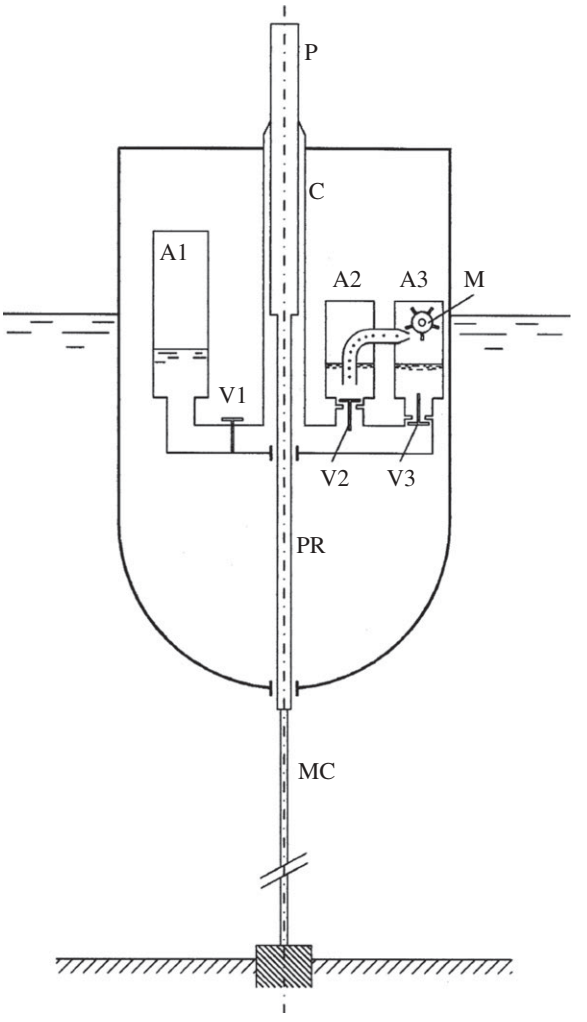

Figure 1. Heaving buoy WEC unit proposed by Budal in 1978 [29, fig. 1]. The machinery consists of a hydraulic cylinder C, three gas accumulators A1, A2 and A3 and three valves V1, V2 and V3. The piston P, with piston rod PR, is connected to a mooring cable MC, pre-tensioned by the pressure in accumulator A1, which also serves discrete-instant phase control when closing or opening the controllable valve V1 at proper instants. The check valves V2 and V3 serve amplitude control and PTO. Hydraulic fluid is discharged at a relatively steady rate from high-pressure accumulator A2 to low-pressure accumulator A3 through a hydraulic motor or Pelton turbine M.

next wave elevation extremum (figures 1 and 2). Note that we may characterize this phase control as latching control only as long as both of the two valves V2 and V3 are closed, which is true as long as the heave amplitude stays too small for either valve to open. Otherwise, it may be said to be a kind of declutching control. Amplitude control, including short-time energy storage, is obtained by means of high-pressure gas accumulator A2 with check valve V2 and low-pressure gas accumulator A3 with check valve V3. Observe that hydraulic fluid can flow only into high-pressure accumulator A2 from the piston pump, and return only

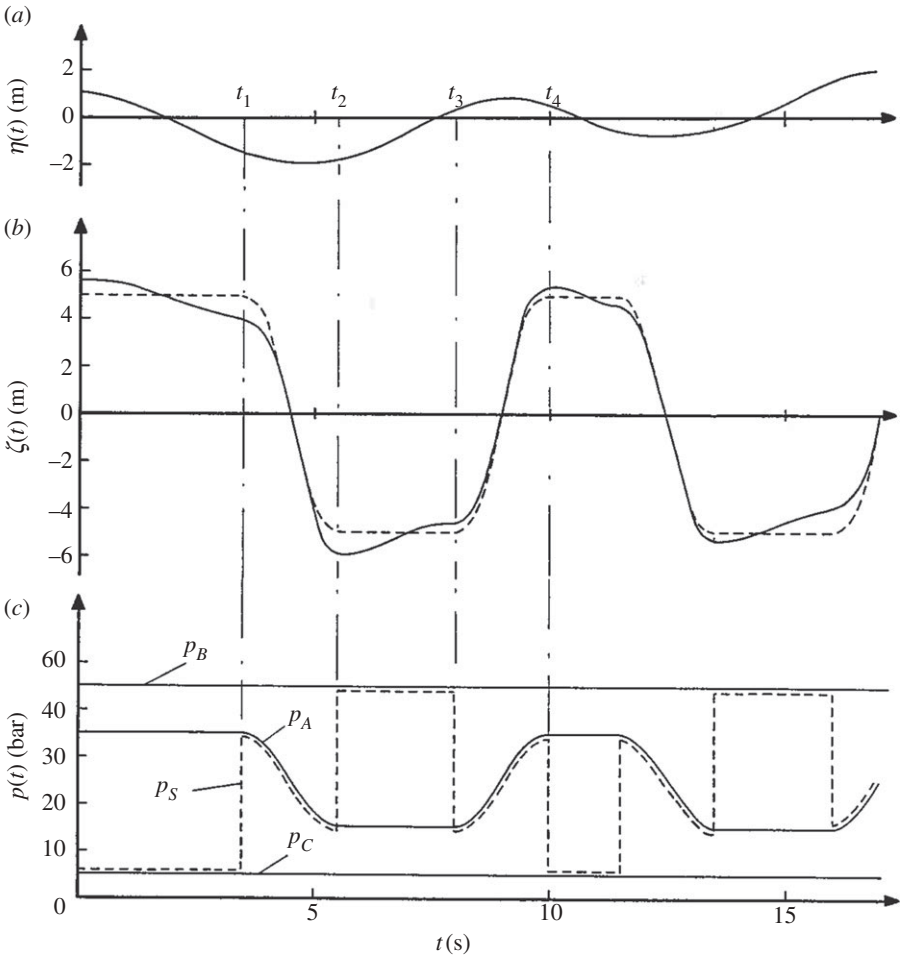

Figure 2. Oscillations with heaving buoy shown in figure 1: (*a*) incident wave elevation $\eta(t)$ at the buoy; (*b*) heave motion $\zeta(t)$ of the buoy, without (dashed curve) or with (fully drawn curve) connection of the hydraulic cylinder C to the gas accumulators A2 and A3 through appropriate opening of check valves V2 and V3; and (*c*) pressures $p(t)$ in the cylinder C (p_S) and in the gas accumulators A1, A2 and A3 (p_A, p_B and p_C respectively). These curves were calculated by Budal [28], assuming that the buoy hull has a diameter of 6 m and cylinder height of 7.5 m, that the piston diameter is 0.62 m, and that gas accumulators A2 and A3 (external to the hull, and common for a group of WEC units) are sufficiently large to keep pressures p_B and p_C constant. The phase-control valve V1 is opened at instants t_1 and t_3 and closed at instants t_2 and t_4.

out from low-pressure accumulator A3. The pressure difference between these two gas accumulators is used to run a hydraulic motor. An even flow of mechanical energy is delivered by the motor's rotating shaft, although fluid-pressure energy is received by the short-time energy store, as lumps from the piston pump, during time intervals when the buoy is near its extreme heave positions. The motor and the energy store (gas accumulators A2 and A3) may, alternatively, be placed outside the buoy hull, e.g. on the sea bed, and connected to an array of WEC units by means of hydraulic hoses.

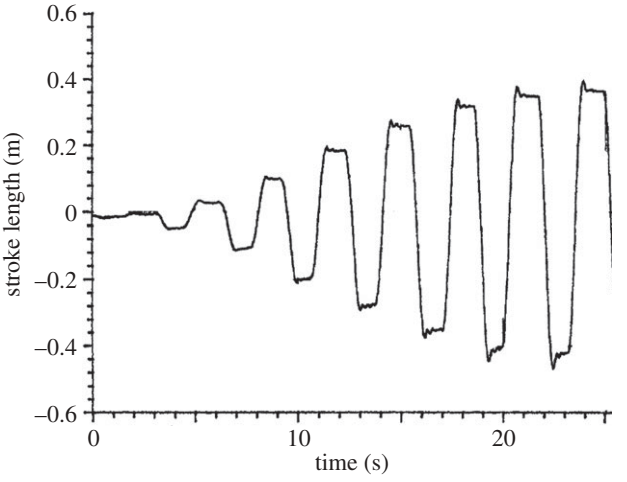

Figure 3. Building up of phase-controlled buoy's heave oscillation to a stroke length of 0.8 m in a wave of height 0.16 m and period 3.1 s [29, fig. 2*b*]. Measurement from a model experiment in a 10.5 m wide wave tank. The model, as indicated in figure 1 (but with gas accumulators A2 and A3 external to the hull), has a diameter of 1.1 m and a cylinder height of 1.4 m.

A buoy model in scale 1 : 6 was tested in 1978 in a wave tank from which a photo and a video clip are available on the Internet [30]. The measured heave motion during the first 25 s after starting operation of valve V1 is shown in figure 3. The incident wave is sinusoidal with wave period 3.1 s and wave amplitude 0.08 m. At each valve-V1-closure instant, a transient vibration is induced in the mooring cable. This may be observed on the experimental graph of figure 3. During the first five to six oscillation cycles, wave energy is fed into the buoy as its heave amplitude has increased to a level where check valves V2 and V3 are no longer closed during the complete cycle. The shape of the experimental heave-stroke curves is essentially in agreement with the simple theoretical curves indicated in figure 2*b*, the fully drawn curve for cycles when check valves V2 and V3 open, and the broken curve for cycles when these valves do not open. Only in this latter case is it appropriate to denote this kind of discrete-instant control as latching control. We may say that the control for the (figure 1) WEC unit is a combination of latching control and declutching control. Unfortunately, in this model experiment, because of fluid leakage and friction in the seals of the piston pump, only a minor fraction (about 0.2) of the absorbed wave energy was delivered to the gas-accumulator energy store [29].

During the late 1980s, it became clear to the wave-energy community that the problem of maximizing wave-power absorption is a non-causal problem [31,32]. This difficulty does not only apply to reactive control, but also to discrete-instant control, as was evident even in 1978. By considering the diagram of figure 2, we note that the opening of valve V1 should take place at about 1 s (about one-quarter of the buoy's natural heave period) before the next extremum of the incident wave elevation. Thus, some online knowledge of the incident wave is required for at least 1 s into the future. If the wave is not sinusoidal, such

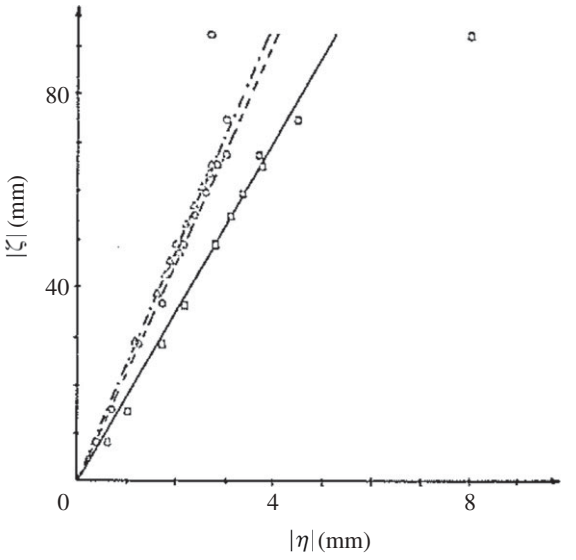

Figure 4. Linearity test of heaving body of diameter 0.15 m and equilibrium draft 0.18 m [33, fig. 4]. Relation between wave amplitude $|\eta|$ and heave amplitude $|\zeta|$. Straight inclined lines are fitted to experimental points in the linear region. For the steepest line, $|\zeta|$ is the input and $|\eta|$ is the response. For the least steep line, $|\eta|$ is the input and $|\zeta|$ is the response.

knowledge is somewhat uncertain. Hence, as prediction procedures to estimate the incident wave future may not be quite correct, the valve V1 cannot always be opened exactly at the ideal instants.

In the quantitative discussion to follow in the subsequent sections, wave and oscillation amplitudes are assumed to be sufficiently small for the hydrodynamic interaction between waves and oscillating systems to be linear. To evaluate the range of validity of such an assumption, it is relevant to keep in mind the result from an experimental linearity test as shown in figure 4 [33]. The test was carried out in a narrow wave channel on a smaller buoy model of shape as the axisymmetric hull shown in figure 1, and it indicates reasonably good linearity as far as the amplitude of the heaving body does not exceed the body's radius of curvature. This corresponds to $K_C = VT/L$ being less than π, where K_C is the Keulegan–Carpenter number [34], T the oscillation period, V the amplitude of the relative fluid velocity along the water-to-body interface and L a characteristic length, which we take to equal the diameter $2a$ of the body.

3. Wave absorption means wave generation

Let us consider a case with a monochromatic plane wave, which is propagating at an angle of incidence β with respect to the x-axis, and which has a wave elevation with complex amplitude

$$\hat{\eta}_0 = A\mathrm{e}^{-\mathrm{i}k(x\cos\beta + y\sin\beta)} = A\mathrm{e}^{-\mathrm{i}kr\cos(\theta-\beta)}, \tag{3.1}$$

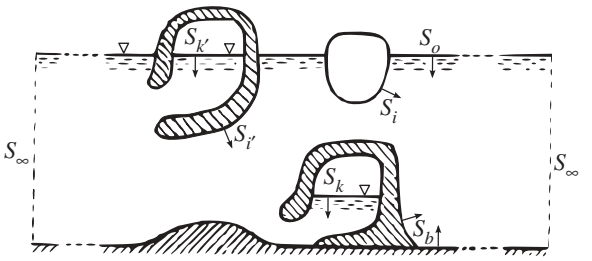

Figure 5. Wave-interacting objects inside an envisaged (control) surface S_∞, chosen as a cylindrical surface $r =$ const. Two floating bodies are indicated, as well as two OWCs, one in a floating structure and the other in a fixed (bottom-standing) structure.

where the horizontal coordinates (x, y) are related to the polar coordinates (r, θ) through $(x, y) = (r\cos\theta, r\sin\theta)$. Furthermore, A is the complex amplitude of the incident wave elevation at $(x, y) = (0, 0)$, and k is the angular repetency (wavenumber), which is related to the angular frequency ω through the dispersion relationship $\omega^2 = gk\tanh(kh)$, g being the acceleration of gravity and h the water depth. The angle of wave incidence β is explicitly introduced, because the coordinate system is assumed to be fixed for the group of WEC units (figure 5), while the direction of incident-wave propagation may be a variable parameter. Before discussing the general WEC system, we shall, as a prelude, consider a single-body WEC.

It is well known that for a single immersed body oscillating in only one of its six modes (degrees of freedom), mode j, say, the time-averaged absorbed power is $P_\mathrm{a} = P_\mathrm{e} - P_\mathrm{r}$, where

$$P_\mathrm{e} = \tfrac{1}{2}\Re[f_j(\beta)A\hat{u}_j^*] = \tfrac{1}{4}[f_j(\beta)A\hat{u}_j^* + f_j^*(\beta)A^*\hat{u}_j] \tag{3.2}$$

is the 'excitation power', which is linearly related to A as well as to the complex velocity amplitude $\hat{u}_j$, and where

$$P_\mathrm{r} = \tfrac{1}{2}R_{jj}|\hat{u}_j|^2 \tag{3.3}$$

is the 'radiated power', which is not explicitly related to A, but quadratic in $\hat{u}_j$. Further, $f_j(\beta)$ is the excitation-force coefficient for mode j, $f_j(\beta)A$ is the excitation force and R_{jj} is the radiation resistance. The asterisk (*) denotes complex conjugate.

A fruitful point of view is to consider a wave energy-absorbing system as a generator of waves that interact with incident waves, such as to reduce the amount of wave energy that is otherwise present in the sea [4]. The system must generate a wave, which interferes destructively with the sea waves. 'In order for an oscillating system to be a good wave absorber it should be a good wave generator' [15]. Let us consider a general system as indicated in figure 5, in which is indicated a group of immersed objects that can interact with waves. There is no such object in the water domain outside the indicated envisaged surface S_∞, which may be of cylindrical shape and of radius r that we may let tend to infinity.

When the incident wave $\hat{\eta}_0$ hits the WEC unit structures inside the control surface S_∞, an outgoing diffracted wave $\hat{\eta}_\mathrm{d}$ is established, even if all oscillation amplitudes are zero. In addition, a radiated wave $\hat{\eta}_\mathrm{r}$ is generated in the case of

non-zero oscillation amplitudes. While the diffracted wave is linearly related to A, the radiated wave is linearly related to all WEC units' oscillation amplitudes. In the far-field region, outside S_∞, the outgoing waves have complex amplitudes as given asymptotically by

$$\hat{\eta}_{\mathrm{d/r}} = \left(\frac{-\mathrm{i}\omega}{g}\right) C_{\mathrm{d/r}}(\theta)(kr)^{-1/2}\mathrm{e}^{-\mathrm{i}kr} + \cdots, \quad \text{as } kr \to \infty, \tag{3.4}$$

where the complex functions $C_{\mathrm{d}}(\theta)$ and $C_{\mathrm{r}}(\theta)$ are the far-field coefficients for the diffracted and the radiated waves, respectively. In certain cases, it is convenient to express these $C_{\mathrm{d/r}}(\theta)$ functions in terms of the so-called Kochin functions $H_{\mathrm{d/r}}(\theta) = \sqrt{2\pi}\, C_{\mathrm{d/r}}(\theta)\mathrm{e}^{\mathrm{i}\pi/4}$.

For a single-body WEC, we may write $C_{\mathrm{r}}(\theta) = c_j(\theta)\hat{u}_j$ and $H_{\mathrm{r}}(\theta) = h_j(\theta)\hat{u}_j$, if the body oscillates in only one mode j of motion. (Otherwise, we have to sum over all relevant j's.) Applying the well-known Haskind relation [35, eqn (45)], the excitation-force coefficient may be written as

$$f_j(\beta) = 2\rho v_{\mathrm{g}} v_{\mathrm{p}} h_j(\beta+\pi) = 2\rho v_{\mathrm{g}} v_{\mathrm{p}} \sqrt{2\pi}\, c_j(\beta+\pi)\mathrm{e}^{\mathrm{i}\pi/4}, \tag{3.5}$$

where ρ is the mass density of water, and where v_{g} and v_{p} are the wave's group and phase velocity, respectively. This Haskind relation is a reciprocity relation between a radiation parameter h_j and a diffraction parameter f_j, both referring to the same oscillation mode j. Next, we apply another reciprocity relation between diffraction and radiation problems, namely [35, eqn (48b)],

$$h_j(\beta+\pi) = h_j^*(\beta) - \frac{\omega}{2\pi g}\int_0^{2\pi} \frac{H_{\mathrm{d}}(\theta)}{A} h_j^*(\theta)\,\mathrm{d}\theta. \tag{3.6}$$

Recalling that $H_{\mathrm{r}}(\theta) = h_j(\theta)\hat{u}_j$, we now define the global excitation parameter

$$E = E(\beta) = \frac{\rho v_{\mathrm{p}} v_{\mathrm{g}}}{2}\left(H_{\mathrm{r}}(\beta) - \frac{\omega}{2\pi g}\int_0^{2\pi} \frac{H_{\mathrm{d}}^*(\theta)}{A^*} H_{\mathrm{r}}(\theta)\,\mathrm{d}\theta\right), \tag{3.7}$$

which, in general, is a complex quantity. Hence, equation (3.2) may be rewritten as

$$P_{\mathrm{e}} = E^* A + E A^* = E^*(\beta)A + E(\beta)A^*. \tag{3.8}$$

Here, the excitation power P_{e} is expressed in terms of far-field wave parameters, in contrast to local mechanical parameters of the wave-interacting body, as in equation (3.2). Also the radiated power P_{r} is expressed by local parameters, R_{jj} and $\hat{u}_j$, in equation (3.3), which is an expression for the power that, in the case of no incident wave, is radiated away from the single body, when it is performing forced oscillation with complex velocity amplitude $\hat{u}_j$. Since we, in the present analysis, assume the water to be an ideal fluid with no energy loss, we expect to find the same radiated power in the far-field region. If we, for this single-mode case, compare equation (3.3) with the last term of the global equation (eqn (61b)) derived by Newman [35], we may rewrite equation (3.3) as

$$P_{\mathrm{r}} = \frac{\omega\rho v_{\mathrm{p}} v_{\mathrm{g}}}{4\pi g}\int_0^{2\pi} |H_{\mathrm{r}}(\theta)|^2\,\mathrm{d}\theta \equiv |D|^2. \tag{3.9}$$

Using equations (3.8) and (3.9), we find the following equation for the power P_a that is absorbed by the, single-mode, oscillating body:

$$P_a = P_e - P_r = (AE^* + A^*E) - |D|^2 = \left|\frac{AE}{D}\right|^2 - \left|\frac{AE^*}{D^*} - D\right|^2, \tag{3.10}$$

as expressed in terms of far-field wave quantities. From equations (3.7)–(3.9), we see that these far-field quantities are the Kochin functions for the diffracted and the radiated waves, in addition to the amplitude of the (undisturbed) incident wave.

From a wave-interference point of view, it is reasonable to assume that equations (3.7)–(3.10) are applicable also for the, more general, situation with a group of WEC units, oscillating bodies, as well as OWCs (figure 5), provided $H_d(\theta)$ and $H_r(\theta)$ are the Kochin functions for the diffracted and the radiated waves, respectively, in this more general situation. That equations (3.7)–(3.10) are, in fact, applicable for this general situation is shown more rigorously in appendix A; see equations (A 11)–(A 13). We may note that, while $|D|^2$ is proportional to the square of the radiated wave's amplitude in the far-field region, $E = E(\beta)$ is linearly related to this amplitude, and it is also a function of β, the propagation direction of the incident plane wave.

Mathematical expressions for the maximum power absorbed by a group of WEC units were derived by Evans [36, eqn (4.3)], Falnes [37, eqn (15)] and Falnes & McIver [38, eqn (29)], considering optimum oscillation of each of the WEC units. In contrast, here we shall find the maximum absorbed power by a global method, that is by considering the total radiated wave in the far-field region. By inspection we see, from the right-hand side (r.h.s.) of equation (3.10), that the maximum absorbed power is $P_{a,MAX} = |AE(\beta)/D|^2$, which is obtained for the optimum condition $AE^*(\beta)/D^* - D = 0$, or $AE^*(\beta) = |D|^2$. From this, it follows that we have several different alternative expressions for the maximum absorbed power:

$$P_{a,MAX} = P_{r,OPT} = |D_0|^2 = \frac{P_{e,OPT}}{2} = AE_0^*(\beta) = A^*E_0(\beta) = |AE_0(\beta)|. \tag{3.11}$$

This maximum removal of energy from the incident wave requires that the radiated wave satisfies the optimum condition

$$\frac{|D_0|^2}{E_0^*(\beta)} = \left[\frac{|D|^2}{E^*(\beta)}\right]_{OPT} = A. \tag{3.12}$$

Observe that at optimum, a condition on the radiated wave's phase is that $E(\beta)$ should have the same phase as A, the (undisturbed) incident wave's complex amplitude at the origin. This corresponds to $E_0(\beta)A^* = E_0^*(\beta)A$ being real and non-negative. As may be seen by considering equations (3.2)–(3.7), this means that $f_j(\beta)A\hat{u}_{j,0}^* = f_j^*(\beta)A^*\hat{u}_{j,0}$ is real and non-negative. Thus, as is well known, for a single heaving body, this phase condition means that the optimum heave velocity $\hat{u}_{j,0}$ is in phase with the excitation force $f_j(\beta)A$, a condition that may be automatically achieved, provided the body is in resonance with the incident wave [3,4,39,40]. This is not, however, so for the case of two, hydrodynamically interacting, heaving bodies [37]. The optimum condition (3.12) is, however, general. In addition to the phase condition, equation (3.12) also implies that

the amplitude of the radiated wave should satisfy $|D^2/E_0(\beta)| = |A|$. For limited volumes of the wave-absorbing (and hence wave-radiating) objects, it will not be possible to satisfy this amplitude condition unless the wave height $H = 2|A|$ of the incident wave is below a certain value.

In equations (3.12) and (3.11), $E_0(\beta)$ and $|D_0|^2$ are optimum values of the radiated wave's global parameters $E(\beta)$ and $|D|^2$, defined by equations (3.7) and (3.9). They correspond to one optimum complex quantity that determines an optimum phase and an optimum amplitude of the radiated wave, and thus to an optimum value $H_{\mathrm{r},0}(\theta)$ of the Kochin function $H_{\mathrm{r}}(\theta)$. We may note that the optimum Kochin function $H_{\mathrm{r},0}(\theta)$ has to satisfy an integral equation (A 14), which is derived in appendix A. (Observe that this optimization does not consider the optimum Kochin function's θ variation, which may be changed, however, by geometrical or structural changes made locally at the wave-interacting oscillating objects indicated in figure 5.) Using equations (3.7) and (3.9), we may rewrite the maximum absorbed power as

$$P_{\mathrm{a,MAX}} = \left| \frac{AE_0(\beta)}{D_0} \right|^2 = \frac{\rho g v_{\mathrm{g}} |A|^2}{2k} G(\beta) = \left(\frac{J}{k} \right) G(\beta) = J d_{\mathrm{a,MAX}}, \tag{3.13}$$

where $J = \rho g v_{\mathrm{g}} |A|^2/2$ is the incident wave-power level and $d_{\mathrm{a}} \equiv P_{\mathrm{a}}/J$ is the 'absorption width' (also called 'capture width', a term that might preferably be reserved for the necessarily smaller ratio between the converted useful power and J). Moreover, we have introduced the gain function

$$G(\beta) = \frac{2\pi |H_{\mathrm{r},0}(\beta) - (\omega/2\pi g) \int_0^{2\pi} [H_{\mathrm{d}}(\theta)/A]^* H_{\mathrm{r},0}(\theta)\, \mathrm{d}\theta|^2}{\int_0^{2\pi} |H_{\mathrm{r},0}(\theta)|^2\, \mathrm{d}\theta}. \tag{3.14}$$

By referring to analogous wave phenomena in atomic and nuclear physics, and in optics, also Farley [41, appendix] derived corresponding global results, as given, for example, by equations (3.10)–(3.14).

For the case of a single body WEC that oscillates in only one mode j, we have $H_{\mathrm{r}}(\theta) = h_j(\theta)\hat{u}_j$, and we define the adjoint Kochin function $\bar{H}_{\mathrm{r}}(\theta) \equiv h_j(\theta)\hat{u}_j^*$, which may differ from $H_{\mathrm{r}}(\theta)$ in phase, but not in magnitude. Applying the reciprocity relation (3.6) to simplify the numerator in the fraction of equation (3.14), the gain function may be written as [42]

$$G(\beta) = \frac{2\pi |\bar{H}_{\mathrm{r},0}(\beta + \pi)|^2}{\int_0^{2\pi} |H_{\mathrm{r},0}(\theta)|^2\, \mathrm{d}\theta} = \frac{2\pi |H_{\mathrm{r},0}(\beta + \pi)|^2}{\int_0^{2\pi} |H_{\mathrm{r},0}(\theta)|^2\, \mathrm{d}\theta}, \tag{3.15}$$

which is the ratio between the value of $|H_{\mathrm{r},0}(\theta)|^2$ in the direction $\theta = \beta + \pi$ (that is, in the direction opposite to the propagation direction of the incident wave) and the value of $|H_{\mathrm{r},0}(\theta)|^2$ averaged over all directions, $0 \le \theta < 2\pi$. From a physical point of view, it might be conjectured that it is irrelevant how the optimum radiated far-field wave is brought about, whether it is by a single-mode single-body radiator, or whether it is by a more general radiating array consisting of oscillating bodies as well as of OWCs. We may thus raise the question as to whether equation (3.15) applies also for the latter system. This matter is discussed to some extent in appendix A, and it is found that only the expression with $\bar{H}_{\mathrm{r},0}$ in the numerator may be generalized.

For an axisymmetric WEC system, it is sufficiently general to consider an incident wave propagating in the x direction, and then $\beta = 0$. If it is radiating isotropically, $H_{\mathrm{r}}(\theta)$ is independent of θ. Then, since $H_{\mathrm{r},0}(\pi) = H_{\mathrm{r},0}(0)$, we may, from equations (3.14) and (3.15), conclude that $\int_0^{2\pi} H_{\mathrm{d}}(\theta)\,\mathrm{d}\theta = 0$ for an axisymmetric WEC system. It follows that for isotropic wave radiation, $G(\beta) \equiv 1$, and we have the well-known result [4,10,35,39] that the maximum absorption width is $d_{\mathrm{a,MAX}} = 1/k = \lambda/2\pi$, where $\lambda = 2\pi/k$ is the wavelength. This corresponds to the optimal interference between a plane incident wave and an isotropically radiated wave on the sea surface. Such an isotropic radiation may be realized by means of an axisymmetric system consisting of a heaving body, an OWC or a submerged pulsating-volume device or by means of a concentric axisymmetric group of such objects. These systems may be described as source-mode wave radiators.

In contrast to a source-('monopole'-)mode radiator, for a dipole-mode radiator, some part of its wave-interacting surface has a positive displacement of water, while another part of the surface has an equally large, but negative, water displacement. Examples of dipole-mode radiators are surging or pitching bodies. As shown by Newman [35], for a pitching or surging axisymmetric body, we have $G(\beta) = 2\cos^2\beta = 2$, and thus $P_{\mathrm{a,MAX}} = 2J/k = J\lambda/\pi$. In this case, $H_{\mathrm{r}}(\theta) = H_{\mathrm{r}}(0)\cos\theta$, and hence $H_{\mathrm{r},0}(\pi) = -H_{\mathrm{r},0}(0)$, which means that the integral in the numerator of equation (3.14) does not vanish for an oscillation mode that radiates anti-symmetrically in the forward and backward directions. We have, however, $|H_{\mathrm{r},0}(\pi)| = |H_{\mathrm{r},0}(0)|$. From equation (3.15), we easily find $G(\beta) = G(0) = 2$.

Further, Newman [35] also showed that $P_{\mathrm{a,MAX}} = 3\,J/k$ for an axisymmetric body that oscillates in both the surge mode, $j = 1$, and the heave mode, $j = 3$. Then, we may write the radiated wave's Kochin funcion as $H_{\mathrm{r}}(\theta) = h_1(\theta)\hat{u}_1 + h_3(\theta)\hat{u}_3 \equiv H_1(\theta) + H_3(\theta)$. From symmetry considerations, it follows that there is no hydrodynamic coupling between these two modes [43, pp. 126–127, 172], and, hence, equations (3.2)–(3.6) are applicable for either mode, separately. Moreover, $H_{\mathrm{r}}(\theta) = h_1(0)\cos(\theta)\hat{u}_1 + h_3(0)\hat{u}_3 = -h_1(\pi)\cos(\theta)\hat{u}_1 + h_3(\pi)\hat{u}_3$. Thus, unless $h_1(\pi)h_3(\pi) = 0$, we have $|H_{\mathrm{r},0}(\pi)| \neq |H_{\mathrm{r},0}(0)|$.

It may, finally, be remarked that if a sufficiently small axisymmetric source-mode wave absorber—a point absorber (PA)—is located a distance b in front of a completely reflecting vertical wall or cliff at the plane $x = 0$, instead of in the open sea, then—assuming that the sea region is $x < 0$ and thus the angle of incidence is in the interval $|\beta| < \pi/2$—there is contribution to the integral in equation (3.15) only from the interval $\pi/2 < \theta < 3\pi/2$. Then, $G(\beta) = 2[1 + \cos(2kb)\sin\beta]/[1 + J_0(kb)]$, where J_0 denotes the Bessel function of first kind and zero order [44]. If $b \to 0$, then $G(\beta) \to 2$ and, consequently, $P_{\mathrm{a,MAX}} \to J\lambda/\pi$, which is twice as large as for a PA in open sea.

4. The Budal diagram: 'dreams and reality'

There exist two upper bounds, P_A and P_B, for the power P that can be absorbed, from a sinusoidal wave of height $H = 2|A|$ and period $T = 2\pi/\omega$, by means of an immersed body, whose maximum swept volume is V. Here, V is defined as twice the amplitude of oscillating water displacement; for a semi-submerged heaving buoy, V is the difference between maximum and minimum displacement. While the P_A bound, which corresponds to the maximum amount of energy that can

be removed from an incident wave, stimulated the dreams of the mid-1970s, the P_B bound indicates how a realistically sized immersed absorber object puts an upper bound to the amount of primary converted wave energy.

The upper power bound P_A corresponds to the maximum absorbed power given by equation (3.11) or (3.13), that is, $P_A = P_{\mathrm{a,MAX}} = P_{\mathrm{r,OPT}} = (1/2)P_{\mathrm{e,OPT}}$, which corresponds to the radiated wave's optimum condition (3.12). This condition implies both the optimum amplitude condition $|D^2/E| = |A|$ and the optimum phase condition that E should be in phase with A. Then a maximum amount of wave energy is removed from the sea.

The second upper power bound, Budal's upper bound, P_B corresponds, however, to a situation where the design swept volume V, but not the wave energy available in the sea, is exploited as much as possible. We observe from equation (3.10) that $P_{\mathrm{a}} = P_{\mathrm{e}} - P_{\mathrm{r}} \le P_{\mathrm{e}} = AE^* + A^*E$, since $P_{\mathrm{r}} = |D|^2$ is non-negative. In accordance with equation (3.2), for a heaving semi-submerged body, the excitation power is $P_{\mathrm{e}} = (1/2)|\hat{F}_{\mathrm{e},3}\hat{u}_3|\cos\gamma_3$, where $\hat{F}_{\mathrm{e},3} = f_3(\beta)A$ and $\hat{u}_3$ are complex amplitudes of the heaving body's excitation force and velocity, respectively, and where γ_3 is the phase angle between these two quantities. Now, $\cos\gamma_3 \le 1$, where equality holds for the case of optimum phase. Budal considered a tall cylindrical body with relatively small water-plane area S_{w}. Then, with optimum phase ($\gamma_3 = 0$), the heave amplitude $|\hat{s}_3|$ may be significantly larger than the wave amplitude $|A|$. Noting that $|\hat{u}_3| < \omega V/2S_{\mathrm{w}}$ and $|\hat{F}_{\mathrm{e},3}| < \rho g S_{\mathrm{w}} A$, he established the inequality

$$|\hat{F}_{\mathrm{e},3}\,\hat{u}_3| \le \frac{\omega\rho g V|A|}{2}, \tag{4.1}$$

where equality may be approached provided the design swept volume V is fully used and provided $V/\lambda^3 \ll 1$. It may be noted that Rainey (R. Rainey 2003, personal communication) derived the same inequality by considering a wave-interacting low cylindrical body with relatively large water-plane area. Then the heave amplitude should not exceed the wave amplitude. Moreover, the excitation force amplitude is bounded by the body's buoyancy force at equilibrium in still water. In this situation, we have $|\hat{u}_3| < \omega|A|$ and $|\hat{F}_{\mathrm{e},3}| < \rho g V/2$, which also leads to the above Budal's inequality (4.1).

Thus, we have the following upper power bound:

$$P_B = \frac{\omega\rho g V|A|}{4} = \frac{c_0 VH}{T}, \tag{4.2}$$

where $c_0 = (\pi/4)\rho g = 7.9\,\mathrm{kW\,m^{-4}\,s}$, as in Budal's original derivation [12, eqn (5.2)], which is based on the assumption of the heave oscillation being sinusoidal. (However, if we allow for full reactive control, an abrupt motion of the body between opposite extreme heave positions, at each instant of extreme heave excitation force, could have been achieved—at least theoretically. In such a case, we could have chosen $c_0 = \rho g = 10\,\mathrm{kW\,m^{-4}\,s}$. In the present paper, we choose, however, to use Budal's own value.) We may note that we have not yet specified a particular geometry for the heaving semi-submerged body. The upper bound (4.2) is even also applicable to an array or a group of such bodies, provided V is the sum of all bodies' design swept volumes.

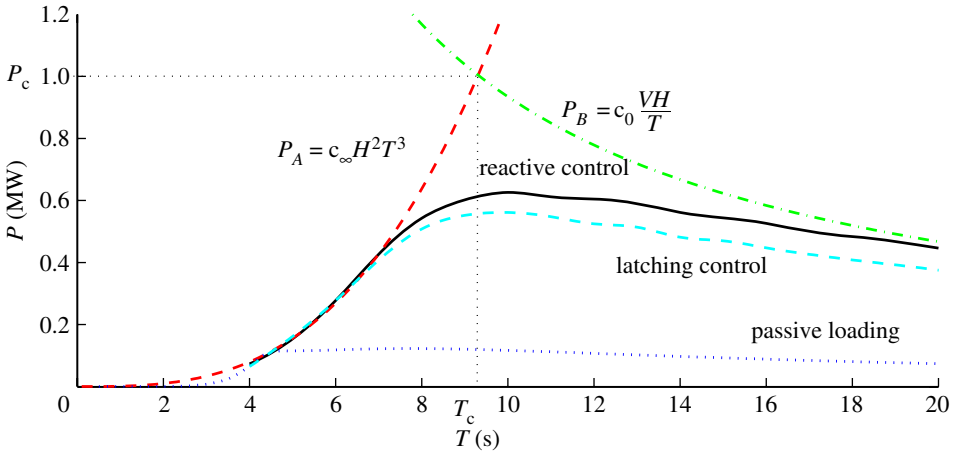

Figure 6. Budal diagram. Two upper bounds, P_A and P_B, for the power P that can be absorbed from a sinusoidal wave of height $H = 2|A|$ and period $T = 2\pi/\omega$ by means of an immersed source-mode axisymmetric absorber of volume V (maximum swept volume). The scales shown for T and P apply for a situation with $H = 2.26\,\mathrm{m}$ and $V = 524\,\mathrm{m}^3$, corresponding to an intersection point $(T_c, P_c) = (9.3\,\mathrm{s}, 1.0\,\mathrm{MW})$. Below the dashed P_A and the dashed-dotted P_B upper bound curves there are three curves that represent the power absorbed by a semi-submerged sphere heaving with optimum amplitude (optimum load), when three different control strategies as indicated are applied [23]. The sphere has a diameter of $2a = 10\,\mathrm{m}$, and its heave amplitude is load-constrained not to exceed 3 m. (Online version in colour.)

In the following discussion, we shall, for convenience, assume deep-water conditions. Thus, we use the dispersion relationship $\omega^2 = gk$, which means that the wavelength $\lambda = 2\pi/k$ and the wave period T are related by $\lambda/T^2 = 1.56\,\mathrm{m\,s^{-2}}$. Moreover, the group velocity is $v_g = g/2\omega = gT/4\pi$. Further, we shall now assume axial symmetry for the heaving semi-submerged body. Using equation (3.13) for this case, we find

$$P_A = P_{a,MAX} = \frac{\rho g v_g |A|^2}{2k} = \rho \left(\frac{gT}{\pi}\right)^3 \frac{H^2}{128} = c_\infty T^3 H^2, \tag{4.3}$$

where $c_\infty = \rho(g/\pi)^3/128 = 245\ \mathrm{W m^{-2} s^{-3}}$. This upper bound cannot be approached unless the optimum condition (3.12) is satisfied. The resonance bandwidth may include all wave periods if V/λ^3 tends to infinity.

The two upper power bounds, as given by equations (4.2) and (4.3), may, in a P-versus-T 'Budal diagram' (figure 6), be illustrated as a monotonically decreasing P_B curve and a monotonically increasing P_A curve. The three other curves, the three P_a curves that have a maximum in the shown T interval of figure 6, represent the power absorbed by a semi-submerged sphere heaving with optimum amplitude (optimum load). For the lowest curve, there is no phase control, whereas for the second and third lowest curves, phase control by the latching method and by the reactive-control method, respectively, has been assumed [23].

The declining upper bound curve $P_B = c_0 VH/T$ is inversely proportional to the wave period T, and proportional to the wave height H and to the maximum swept volume V of the oscillating object. Contrary to this declining curve, the increasing upper bound P_A curve is dependent on the object's geometry (cf. equations (3.13)–(3.15)). For a symmetric two-dimensional object and for an axially symmetric three-dimensional object, P_A is proportional to T and to T^3, respectively [35]. For non-symmetric objects, as well as in non-deep water cases, the dependence on T is less simple. In all cases, P_A is proportional to H^2, the wave height squared. For a three-dimensional axisymmetric source-mode absorber (e.g. a heaving buoy), the P_A curve shown in figure 6 is applicable. Note that the P_B curve is an upper bound for all kinds of WECs. Lower bounds may be found, however, in some cases, for instance for a dipole-mode absorber, as shown by an example below (in §6).

The capacity of the PTO machinery should be chosen to be lower than the power value P_c corresponding to the intersection point of the two upper bound curves P_A and P_B for some particular combination of H and V, which somehow should be related to a wave climate. How much lower should the power capacity be? This is the matter that is to be discussed in §5. We presume it to be an advantage that the wave climate, the physical WEC volume, the design swept volume V and the installed PTO machinery match reasonably well with each other.

Observe that for each (H, V) combination, there is a different set of upper bounds P_A and P_B. It is convenient to introduce normalized (dimensionless) variables

$$(T_\mathrm{n}\ V_\mathrm{n}\ H_\mathrm{n}\ P_\mathrm{n}) = \left(\frac{T}{(L/g)^{1/2}}\ \frac{V}{L^3}\ \frac{H}{L}\ \frac{P}{\rho g^{3/2} L^{7/2}} \right) \tag{4.4}$$

for time, volume, wave height and power, respectively, where L is a chosen parameter of dimension length. Then the upper bounds are, for axisymmetric source-mode absorbers, $P_{A,\mathrm{n}} = T_\mathrm{n}^3 H_\mathrm{n}^2/(128\pi^3)$ and $P_{B,\mathrm{n}} = (\pi/4)\, V_\mathrm{n} H_\mathrm{n}/T_\mathrm{n}$ in dimensionless quantities. The length parameter L may be chosen, for instance, as the variable wave height H, or as $H_\mathrm{ch}^{\mu} \lambda_\mathrm{ch}^{\nu}$, where $\mu + \nu = 1$ (e.g. $\mu = 1/3$ and $\nu = 2/3$), and where H_ch and λ_ch are the height and the wavelength of a chosen characteristic wave. If L is chosen as H, the corresponding normalized Budal diagram has only one common $P_{A,\mathrm{n}}$ bound, but a separate $P_{B,\mathrm{n}}$ bound, for each different value of V. However, if we, as in the, alternatively, normalized Budal diagram of figure 7, chose L as the radius a of the immersed axisymmetric absorber, then there is a new set of upper bounds for different wave heights H. But with given geometrical proportions, and thus with $V_\mathrm{n} = V/a^3$ independent of the absolute volume size V, the normalized upper bounds do not vary with V.

The upper power bounds are shown as contour lines in a HT coordinate system in figure 8, for a heaving semi-submerged axisymmetric body of volume $V = 300\,\mathrm{m}^3$. $P_B = c_0 VH/T$ is given by a set of straight contour lines—marked with (100 kW, 300 kW, etc.)—in the right-hand part of the diagram, while $P_A = c_\infty T^3 H^2$ is given by a corresponding set of continued, curved contour lines in the left-hand part of the diagram. The two sets of contour lines join at the dashed-and-dotted curve, which corresponds to $P_B = P_A$, that is $H = (c_0/c_\infty)\, V/T^4$.

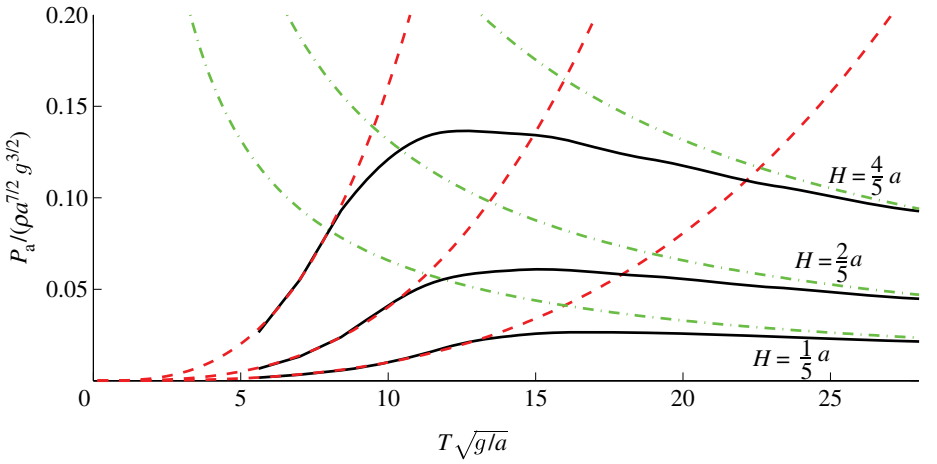

Figure 7. Normalized Budal diagram for a semi-submerged heaving axisymmetric body with normalized volume $V_n = V/a^3 = 4\pi/3$ for three different wave heights, for which the normalized values $H_n = H/a$ are 0.2, 0.4 and 0.8. The upper bounds $P_{A,n}$ and $P_{B,n}$ are shown by the ascending dashed curves and by the descending dash-dotted curves, respectively. The fully drawn curves show the normalized absorbed power $P_{a,n}$, as obtained by numerical optimization assuming application of reactive phase control and optimal loading when the body is a sphere, for which the heave amplitude is being limited to $0.6a$. (Online version in colour.)

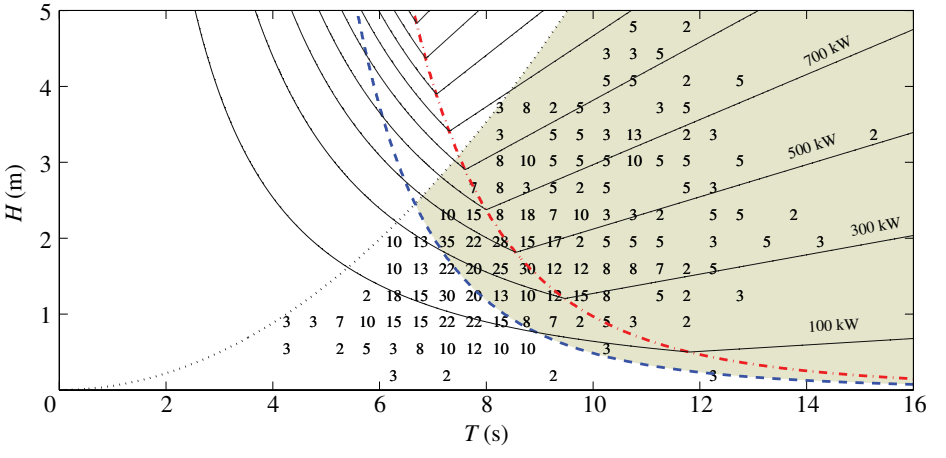

Figure 8. Set of contour lines (100 kW, 300 kW, etc.), in the TH plane, showing upper bounds P_A or P_B for wave power absorbed by a semi-submerged heaving axisymmetric body of volume $V = 300\,\mathrm{m}^3$. The contour lines are ascending straight P_B lines and descending curved P_A lines on the r.h.s. and l.h.s., respectively, of the intersection curve, shown by the dashed-and-dotted line, where $P_A = P_B$. The shaded area above the dashed curve indicates the region $P_B < 2P_A$, where the heave amplitude has to be constrained corresponding to the maximum swept volume V. In the region $H\sqrt{2} > \lambda/20 = (0.055\,\mathrm{m\,s^{-2}})\,T^2$, above the dotted parabola, real sea waves are hardly seen, owing to wave breaking. The numbers written in the area below the parabola are per-thousand wave-state observations at South Uist [45, p. 80], but with T_e and H_s intervals replaced by intervals of T and $H\sqrt{2}$. (Online version in colour.)

In figure 6, the two upper bound curves P_A and P_B intersect at a point (T_c, P_c). By solving the equation $P_A = P_B$, we might express T_c and P_c in terms of H and V, but here we now prefer to express P_c and V in terms of T_c and H as

$$P_c = c_\infty H^2 T_c^3 \quad \text{and} \quad V = \left(\frac{c_\infty}{c_0}\right) H T_c^4 \tag{4.5}$$

or, correspondingly, $P_{c,n} = T_{c,n}^3 H_n^2/(128\pi^3)$ and $V_n = H_n T_{c,n}^4/(32\pi^4)$ in normalized quantities—because we consider such expressions to be very useful when selecting reasonable sizes for the installed power capacity and for the swept volume of a WEC unit of source-mode type.

5. Selection of wave energy converter size and power take-off capacity

Let us here illustrate such a selection by the following example, which we shall base on consideration of a T_e–H_s scatter diagram for the Scottish wave energy resource at South Uist [46] (reproduced by Shaw [45, p. 80]). The observation per-thousand-number entries in this scatter diagram are written into the HT coordinate system of figure 8, with the energy period T_e and the significant wave height H_s replaced by T and $H\sqrt{2}$, respectively. Note that there is hardly any observation above the shown dotted parabolic curve corresponding to $H = 0.035\,T^2 g/(2\pi)$, or $H\sqrt{2} = \lambda/20$. We find that the most frequent wave states have a significant wave height H_s in the region 1.5–3 m with energy period T_e in the region 7–9 s. Moreover, we find that the wave power level J exceeds $40\,\mathrm{kW\,m^{-1}}$ about one-third of the year. Assuming that, in order to be commercially viable, a WEC should work at full capacity at least one-third of the time, the size of the WEC unit and the installed power capacity should match wave power levels up to no more than $40\,\mathrm{kW\,m^{-1}}$. For a sinusoidal wave of period $T = 8$ s, say, this wave power level corresponds to a wave height of $H = 2.26$ m (that is, significant wave height $H_s = H\sqrt{2} = 3.2$ m). Looking at figures 6 and 7, it then seems reasonable to choose $T_c = T = 8$ s. With these numbers, equations (4.5) give $P_c = 640$ kW and $V = 287\,\mathrm{m^3} \approx 300\,\mathrm{m^3}$ for the case of an axisymmetric WEC.

For wave periods in the range of 7–20 s, the latching-control curve in figure 6 indicates an absorbed power P_a about one-half of P_c. For reactive control, the corresponding power ratio P_a/P_c is somewhat higher, and varies between 0.58 and 0.65 for the four reactive-control curves shown in figures 6 and 7. These findings indicate that a power capacity in excess of 300–400 kW should not be chosen for any axisymmetric WEC deployed in a wave climate as off the Scottish coast at South Uist, where we have chosen to design for a wave of height $H = 2.26$ m and period $T = 8$ s. We note from figure 6 that the reactive-control curve follows the P_A curve up to $T = 6.8$ s and $P = 390$ kW. Beyond this point (corresponding to $P_A = P_B/2$), where the reactive-control P_a curve leaves the P_A upper bound curve, the design swept volume is fully used [23]. The shaded area in the diagram of figure 8—applicable for $V = 300\,\mathrm{m^3}$—corresponds to conditions where finite-volume constraints apply, namely for situations where $P_A/P_B > 1/2$ [23], that is $H > c_0/(2c_\infty)\,V/T^4$, which is the area above the dashed

line in figure 8, the scatter diagram of which indicates that for almost all observations with the design wave height, $H = 2.26\,\mathrm{m}$, the design swept volume is fully used.

The passive-loading curve in figure 6 indicates a rather constant absorbed power for a wide range of wave periods around T_c. When the semi-submerged body is a sphere of radius $a = 4.09\,\mathrm{m}$ and volume $287\,\mathrm{m}^3$, the absorbed power for passive loading is about 15 per cent of P_c. This power ratio, $P_a/P_c = 0.15$, would correspond to a required power capacity of about 100 kW. Although the sphere diameter is 8.2 m, the heave stroke length is not more than 1 m, when the incident wave height is $H = 2.26\,\mathrm{m}$. The power ratio P_a/P_c is much more dependent on geometrical ratios for the case with passive loading than with phase control. With passive loading, the power ratio is 19 per cent, 10 per cent and 6 per cent for H/a equal to 0.8, 0.4 and 0.2, respectively, when the semi-submerged heaving axisymmetric body is a sphere. We find that, with passive loading, and with a sphere of radius $a = 9.4\,\mathrm{m}$ and volume $3500\,\mathrm{m}^3$, a power of 300 kW may be absorbed in a wave of height $H = 2.26\,\mathrm{m}$ and period $T = 8\,\mathrm{s}$. Only a very small fraction of this physical volume is used as a swept volume for the required wave interaction. The object of the large physical volume is to change the WEC dynamics in order to compensate for lack of phase control. In contrast, as shown above, a physical volume of $300\,\mathrm{m}^3$, only, is sufficient to match a PTO with a capacity of 300 kW, provided phase control is applied.

Let us now compare the single axisymmetric WEC, which was discussed in the last few paragraphs above, with WECs of a different geometry, but with the same total swept volume V. Firstly, we compare with a WEC consisting of two heaving PA units, and, secondly, with a two-dimensional heaving terminator. In both cases we shall, for simplicity, assume that the WEC is deployed along the y-axis and that $\beta = 0$. Thus, normal wave incidence is assumed.

Suppose that the two PA units are centred at $(x, y) = (0, \pm b/2)$ and that we may neglect effects of wave scattering interaction between the two PA units. Then, according to Budal [47, eqn (37)], Evans [36, eqn (4.13)] or Falnes [37, eqns (47) and (50)], the P_A value for the axisymmetric single-unit case has to be multiplied by $2q_2(0) = 2q_2(\beta)|_{\beta=0} = 2/[1 + J_0(kb)]$, where J_0 is the Bessel function of first kind and zero order. Hence, for this two-body case, the upper power bound becomes $(P_A)_2 = P_A 2q_2(0) = 2c_\infty T^3 H^2/[1 + J_0(4\pi^2 b/gT^2)]$. Note that, as was to be expected, $2q_2(0)$ tends to 1 or 2 as kb tends to zero or infinity, that is, as T tends to infinity or zero, respectively. Moreover, $2q_2(0)$ (which is ≥ 1) has a maximum value of 3.3, approximately, for $kb \approx 3.8$, and otherwise an infinite, but numerable, number of local minima and maxima. For a case with $b = 30\,\mathrm{m}$, the fully drawn, bumpy curve shown in figure 9 represents the upper power bound $(P_A)_2$ for the considered two-PA WEC when the wave is normally incident ($\beta = 0$). As $q_2(0) > 1$ in the interval $2.4048 < kb < 5.5201$, where $J_0(kb)$ is negative, and we thus have $(P_A)_2 > 2P_A$ in the interval $7.1\,\mathrm{s} > T > 4.7\,\mathrm{s}$, there is clearly a profitable constructive interference within this typical region for ocean wave periods. For larger values of the distance b, the bumps on the $(P_A)_2$ curve will come closer together. For arbitrary angles of incidence, the found value of $(P_A)_2$ for $\beta = 0$ has to be multiplied by $q_2(\beta)/q_2(0) = [1 - J_0(kb)\cos(kb\sin\beta)]/[1 - J_0(kb)]$, from which we may find, for example, that $q_2(\pi/2) < 1$ in an infinite, but numerable, number of intervals, $2.4 < kb < 4.4$, $5.5 < kb < 7.7$, …, approximately [37, eqn (50) and fig. 2].

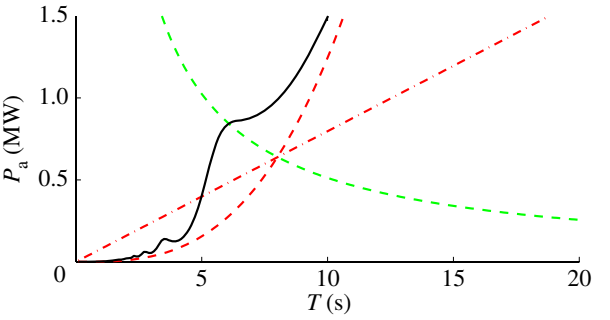

Figure 9. Upper power bounds for—source-type radiating—heaving WEC of total swept volume $V = 287\,\mathrm{m}^3$ when the incident wave height is $H = 2.26\,\mathrm{m}$. The declining dashed hyberbolic curve shows the Budal upper bound, which is common for the three different cases considered. The three other curves (dashed/dash-dotted/fully drawn) show maximum power absorbed from the incident plane wave if the constraint of the limited swept volume is not taken into consideration. The three cases are: case 1 (dashed), single axisymmetric body; case 2 (dashed-dotted), a $\lambda_c/\pi = 32\,\mathrm{m}$ long portion of an infinitely long, symmetrically radiating, line absorber, a heaving terminator; case 3 (fully drawn), two PAs, with centre-to-centre spacing $b = 30\,\mathrm{m}$, and each with a maximum swept volume $V/2$. For cases 2 and 3, the most favourable angle of wave incidence, $\beta = 0$, has been assumed. (Online version in colour.)

Thus, within the corresponding wave-period intervals, which are, approximately, $7.1\,\mathrm{s} > T > 5.2\,\mathrm{s}, 4.7\,\mathrm{s} > T > 4.0\,\mathrm{s}$, ..., we have $(P_A)_2 < 2P_A$ for $\beta = \pi/2$. This drawback may be of minor significance at sites having a wave climate where the predominant wave direction is close to $\beta = 0$. It may be noted, firstly, that the optimum condition (3.12) corresponds to optimum heave velocity having the same phase as the heave excitation force for both PA units, and, secondly, that $(P_A)_2$, which equals the maximum absorbed power (3.11) for this 2-PA-unit WEC, is equally divided between the two PA units, when $\beta = 0$, but not, in general, when $\beta \neq 0$ [37]. It may be of interest to remark that if the volume for either PA unit is increased from $V/2$ to V, then the Budal upper bound P_B will increase by a factor of 2, that is, the declining P_B curve in figure 9 should be lifted to twice the height, while the fully drawn, bumpy upper bound $(P_A)_2$ curve should remain unchanged.

Still assuming $\beta = 0$, we next consider a symmetric, source-mode radiating, two-dimensional WEC of the terminator type. For a portion of width d and of corresponding maximum swept volume V, the increasing P_A curve in figure 6 should be replaced by a straight line, represented by $P_{A'} = Jd/2 = \rho g H^2 v_g d/16 = \rho g^2 H^2 Td/64\pi = (491\,\mathrm{W m^{-3}\,s^{-1}}) H^2 Td$ [35,39,40]. Such a straight line upper bound $P_{A'}$ curve is shown by the dash-and-dotted line in figure 9, where we have chosen $d = \lambda_c/\pi = 32\,\mathrm{m}$, for which value the $P_{A'}$ curve for this two-dimensional terminator portion has the same intersection point with the P_B curve as the P_A curve for the single three-dimensional axisymmetric WEC—of equally large swept volume, $V = 287\,\mathrm{m}^3$—has. From a hull structural point of view, it seems more preferable to design an axisymmetric PA hull of this volume size, such as a sphere of diameter $2a = (6V/\pi)^{1/3} = 8.2\,\mathrm{m}$, rather than a long two-dimensional structure of cross section $V/d = 287/32 = 9.0\,\mathrm{m}^2$. It appears from figure 9 that, at least for normal wave incidence ($\beta = 0$), it is a better option to spend the volume $V = 287\,\mathrm{m}^3$ on two heaving PAs than on a heaving terminator.

6. Point absorbers and quasi-ones: 'small is beautiful'

In the UK wave energy programme that started in the mid-1970s, different types of long WEC structures were investigated [48]. The lengths of such structures were chosen to be of the order of magnitude at least one wavelength. In contrast to these long WEC structures, which we may call line absorbers (or terminators and attenuators according to their orientation relative to the predominant direction of wave propagation), Budal & Falnes [4] proposed much smaller WEC units and introduced the notion of PAs, which were more precisely specified by Count [49] 'as structures that are small in comparison to the incident wavelength (say less than one-twentieth of a wavelength) and are arranged as arrays with no structural connection between adjacent devices'. Let the horizontal extent of each WEC unit be denoted as $2a$. Moreover, the wavelength is $\lambda = 2\pi/k$. Then for the unit to be a PA, according to the original definition, it is required that $ka \ll \pi$ (or, following Count's suggestion, $ka < \pi/20 \approx 1/6 \approx 0.2$). While a terminator, being aligned perpendicularly to the incident wave propagation direction, may to a reasonably good approximation be modelled as a two-dimensional WEC, a PA is definitely an example of a three-dimensional WEC. Apparently, some authors, e.g. Pizer [50] or McCabe & Aggidis [51], seem to have adopted to use PA as a synonym for a three-dimensional WEC. However, if there is a need for another category to bridge the gap between point and line absorbers, we could suggest a term 'quasi-point absorber' (QPA).

For a source-mode WEC, the swept volume cannot be larger than the physical WEC volume. It seems that such a restriction does not apply for a dipole-mode WEC. However, in order to avoid viscous separation, the Keulegan–Carpenter number ought not to be larger than π (see also figure 4). Thus, it will not be practical to operate the WEC by a swept volume V significantly larger than its physical volume. For an oscillating device of such a small size as a PA, dipole-type modes of oscillation (e.g. surge and pitch) are less efficiently interacting with waves than source-type ones, such as a submerged pulsating-volume body, an OWC or a surface-piercing body using the heave mode. For a semi-submerged sphere, for instance, the maximum absorbed power is much larger in heave than in surge for all of the interval $ka < 0.2$ [50]. This is also in agreement with figure 10, which shows that, for a given wave amplitude, larger power is absorbed by the semi-submerged sphere in heave than in surge, when $T\sqrt{g/a} > 10$. This corresponds to $ka = \omega^2 a/g < 0.39$, which is in agreement with Pizer [50, cf. figs 2 and 3]. As shown in figure 10, the upper bound $P_{A,\mathrm{surge}}$ for surge is a factor of 2 larger than P_A for heave [35], but the upper bound $P_{B,\mathrm{surge}} = \rho V a \omega^3 H/3$ for surge [52] is significantly lower than P_B for heave. A physical reason for this is the following. If the body size is reduced to approach a 'point' ($ka \to 0$), the dipole-type modes perform very much poorer as wave generators/absorbers than source-type modes do. All of the oscillating object's wave-generating surface cooperates in displacing water if a source mode is applied. Contrarily, with a dipole mode, a positive water displacement is counteracted by a nearby negative one.

In spite of these observations and the above traditional definition of PA, some authors, regrettably, term their three-dimensional WEC a 'point absorber' also when a dipole-mode oscillation is used. For instance, McCabe & Aggidis [51] investigate an immersed body of width 20 m and draft 20 m, oscillating in the

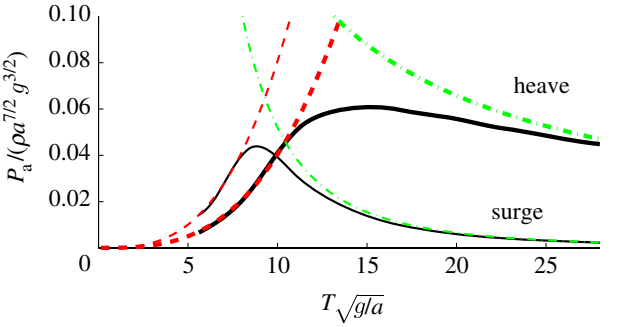

Figure 10. Normalized Budal diagrams, showing upper bounds P_A (dashed lines) and P_B (dashed-dotted lines), for a semi-submerged sphere with normalized volume $V_n = V/a^3 = 4\pi/3$ in wave of normalized height $H_n = H/a = 2/5$ for heave (thick lines) and for surge (thin lines). The fully drawn curves show the normalized absorbed power $P_{a,n}$ when the body is a sphere of radius a and there is reactive phase control, as well as amplitude control by optimum load damping under the constraint that the heave amplitude is being limited to $0.6a$. (Online version in colour.)

surge and pitch modes. Thus, with $a = 10\,\mathrm{m}$, we have, for wave periods $T = 2\pi/\omega$ in the region $6\,\mathrm{s} < T < 12\,\mathrm{s}$, that $1.12 > ka = a\omega^2/g > 0.28$. Thus still $ka < \pi$, but not $ka \ll \pi$. Accordingly, for the actual interval of wave periods, their investigated three-dimensional body is not a PA, but a QPA.

A PA in the form of a completely submerged heaving body is an isotropic wave radiator if it is axisymmetric. However, it does not use its swept volume so well as a heaving semi-submerged buoy, because the submerged body's upper portion's swept volume is partly counteracted by the lower portion's swept volume of opposite polarity. This opposite swept volume will have negligible influence on wave generation, provided the body has such a large vertical extension that the lower swept volume is deep enough to not interact with waves on the water surface. In such a case, however, very little of the body's physical volume can be used as a wave-generating swept volume. Monotonic upper bound curves, as in figures 6 and 7, as well as the thicker monotonic curves in figure 10, are then applicable. But regarding the P_B curves, it should be emphasized that V should be interpreted as the submerged body's upper portion's swept volume. If contrarily, the submerged heaving body is small, including its vertical extension, then it is as poor a wave generator as if it were oscillating in the dipole-type surge mode. We suspect that it then ought to be possible to find a lower upper bound than Budal's original upper bound, the thick monotonic declining curve in figure 10, but instead a lower upper bound, perhaps closer to the thinner monotonic declining curve, derived for the surge mode. From this discussion, we may suggest that a completely submerged PA ought to be of the pulsating-volume type, such as the so-called Archimedes wave swing device [53].

For a heaving cylindrical buoy, the natural frequency $\omega_0 = 2\pi/T_0$—at which resonance with the wave may occur—decreases with increasing draft and radius. Here, the larger of the two length parameters plays the most dominating role. For a semi-submerged sphere of radius a, we may derive that resonance corresponds to $k_0 a = \omega_0^2 a/g = 1.05$ or $\omega_0 = 1.025\sqrt{g/a}$, and that the relative resonance bandwidth is $(\Delta\omega)_{\mathrm{res}}/\omega_0 = \alpha 0.17$ [43, pp. 8, 133, 185, 191], where the factor $\alpha \geq 1$ accounts for load resistance added to the radiation resistance. When the load resistance

equals the radiation resistance, we have $\alpha = 2$, as is the optimum-load situation in cases without amplitude constraint but with optimum phase (e.g. at resonance). In cases with non-optimum phase or with amplitude constraints, a substantially larger load resistance may be required, corresponding to $\alpha \gg 2$; see for example the passive-loading curve in figure 6, for which, with $a = 5.0\,\mathrm{m}$, resonance occurs for $T_0 = 2\pi/\omega_0 = 4.4\,\mathrm{s}$. For the semi-submerged sphere, the natural frequency ω_0 as well as the resonance bandwidth $(\Delta\omega)_{\mathrm{res}}$ are inversely proportional to the square root of the radius a. Similar results have been reported by Garnaud & Mei [54] who analysed a heaving flat-bottomed cylinder of draft equal to the radius a, but considered the case with $\alpha = 2$, only. They found resonance for $k_0 a \approx 0.65$. Because of the larger volume, and hence larger mass, it is reasonable that this $k_0 a$ value is lower than that of the semi-submerged sphere of the same draft and radius a. For such high values of ka, the considered bodies are QPA devices, which would interact better with the wave if operated in the surge mode rather than in the heave mode. That the considered heaving buoy is not a PA, but a QPA, is also illustrated by the following PA-incorrect statement by Garnaud & Mei [54, §2.5]: 'The bandwidth increases as the size of the buoy decreases'. This statement may be correct for a QPA. For a spherical PA buoy (with $ka < 0.2$), however, the bandwidth decreases as the size of the buoy decreases.

For a floating vertical cylinder with a hemispherical bottom—as the one tested with results shown in figure 4—heave resonance occurs for $\omega_0 = 2\pi/T_0 \approx \sqrt{g/b}$ if the draft b is substantially larger than the radius a. Then, in contrast to the semi-submerged sphere, the relative bandwidth $(\Delta\omega)_{\mathrm{res}}/\omega_0$ depends on the geometrical parameters; it decreases strongly with increasing draft. For such a PA cylinder (with $k_0 a < 0.2$), it is possible to obtain resonance within the typical frequency spectrum for ocean waves. The bandwidth is, however, disappointingly small. Hence, it is indispensable to use some kind of optimal or sub-optimal control with such a PA device.

7. Conclusion

It is a fruitful point of view to consider wave absorption as the interference between an incident wave and a radiated wave that is generated by the absorbing device, in such a way that the resulting wave contains less energy than the original incident wave. Wave generation occurs when the oscillatory motion of an immersed object displaces water corresponding to the swept volume of the oscillating object (oscillating body or OWC). In order to have an efficient utilization of the swept volume, we have, in this paper, mainly considered oscillating bodies, which have very small size relative to predominant wavelengths, and which are source-type wave generators. In particular, we have dealt with heaving buoys, including PAs.

To bridge the gap between point absorbers and line absorbers, such as terminators and attenuators, we have proposed a new category, namely QPAs, to which belong several projected three-dimensional WECs that essentially use surge or pitch modes of oscillation, and thus are dipole-type wave generators.

In the hope to promote the future prospects for wave-energy utilization, we have suggested as a design principle that a WEC's PTO capacity, its maximum swept volume and preferably also its full physical volume should be reasonably well matched with the wave climate. To analyse this matter, we have introduced

and applied a diagram that we have denominated as a 'Budal diagram'. It contains two, different, upper bounds for the power that it is possible to absorb from a sinusoidal wave of height H and period T by means of a WEC of given geometry and mode of oscillation and of given maximum swept volume V.

Based on the mentioned design principle, we conclude that, for each WEC unit, the capacity of the installed PTO machinery should not exceed about 300 kW, and that the maximum swept volume should be about 300 m^3. With these design specifications, matching to a typical wave climate, as at South Uist in Scotland, is possible provided the unit is equipped with means for phase control and amplitude control. If a WEC unit of this size does not have phase control, but only passive loading, then the installed power capacity should not be more than about 100 kW. The capacity may, however, be extended to about 300 kW provided the immersed heaving WEC unit has a 10-fold larger physical volume, of which, unfortunately, only a small fraction is used as a wave-generating swept volume.

Hence, a reasonably sized wave-power plant should consist of an array of many (hundreds, or even thousands) power buoy units. It has been suggested, many years ago [55], that 'a 100 MW wave power plant should consist of 1000 units each of capacity 0.1 MW rather than 200 units of capacity 0.5 MW'. In the future, construction of arrays may profit from mass production of many equal units! A prerequisite is, however, the more urgent challenge that consists in developing and demonstrating a prospective single viable WEC unit of power capacity not more than 0.3 MW. If a feasible control technology to optimize the phase and the amplitude of the oscillatory motion can be developed, then each unit of a wave plant array could have a capacity of up to 0.3 MW, according to findings in the present paper.

As a basis for this, we applied frequency-of-occurrence statistics for significant wave heights at South Uist. This characterizes the so-called 'wave states', and thus the corresponding duration curves have a three-hour time resolution. It would have been better to apply as basis occurrence statistics for individual wave heights and wave periods, which would require wave statistics of time resolution not longer than a few seconds.

We wish to devote this paper to the memory of Kjell Budal (1933–1989), who in 1973 initiated wave-power research at the university in Trondheim, and who proposed various WEC devices [29], being always aware of the fact that any wave-absorbing body has to radiate waves interfering in an optimum manner with incident waves. In 1975, he contacted the company Kværner Brug AS, who during several years cooperated with us in developing a phase-controlled power buoy [56]. Kværner Brug AS's very skilled mechanical designer Nils Ambli (1933–1999) expressed to us that our result that the maximum absorption width is $\lambda/2\pi$ for a PA may be interpreted as corresponding to optimum interference of a circular radiated wave with a plane incident wave. Thus, Ambli and Budal's understanding of wave-energy absorption is an inspiration for the development presented in §3 above and in appendix A below. Finally, we also wish to acknowledge Francis Farley for many fruitful discussions on this matter after the turn of the millennium.

Appendix A. Far-field view on wave-energy absorption

The power that is being absorbed from an incident plane wave by means of a WEC system, which is composed of a finite group of individual WEC units, was, about three decades ago, analysed in terms of wave-excitation parameters and oscillation state parameters for each of the individual WEC units [36–38]. In contrast, we

shall here analyse wave-power absorption by considering the interaction between the incident plane wave and the radiated circular wave in the far-field region outside the finite region where all WEC units are located, that is, outside the envisaged cylindrical control surface S_∞, indicated in figure 5. Such a global point of view was applied by Newman [35] and by Farley [41] for a single WEC unit, and, moreover, Budal [47] applied the same global method to analyse the wave power absorbed by a group of wave-absorbing oscillating bodies. In the present analysis, the WEC system may also, in general, contain OWCs.

Making the usual assumptions of an incompressible, irrotational and ideal fluid and of linearity, we consider a monochromatic (sinusoidal) wave, whose wave elevation has a complex amplitude

$$\hat{\eta} = \hat{\eta}_0 + \hat{\eta}_\mathrm{d} + \hat{\eta}_\mathrm{r}. \tag{A 1}$$

It is a superposition of a plane incident wave

$$\hat{\eta}_0 = A\mathrm{e}^{-\mathrm{i}k(x\cos\beta + y\sin\beta)} = A\mathrm{e}^{-\mathrm{i}kr\cos(\theta-\beta)} \tag{A 2}$$

propagating at an angle of incidence β with respect to the x-axis, and an outgoing circular wave

$$\hat{\eta}_\mathrm{d} + \hat{\eta}_\mathrm{r} = \frac{-\mathrm{i}\omega}{g\sqrt{2\pi}}\mathrm{e}^{-\mathrm{i}\pi/4}[H_\mathrm{d}(\theta) + H_\mathrm{r}(\theta)](kr)^{-1/2}\,\mathrm{e}^{-\mathrm{i}kr} + \cdots, \tag{A 3}$$

where the three dots $(\cdots)$ indicate 'near-field' terms, which—in comparison with the explicitly written 'far-field' term—are negligible when $kr \to \infty$. The horizontal coordinates (x, y) are related to the polar coordinates (r, θ) through $(x, y) = (r\cos\theta, r\sin\theta)$. A is the complex amplitude of the incident wave elevation (referred to the origin $r = 0$), and k is the angular repetency (wavenumber), which is related to the angular frequency ω through the dispersion relationship $\omega^2 = gk\tanh(kh)$, g being the acceleration of gravity and h the water depth. The outgoing wave has, in general, two contributions due to diffraction and radiation, denoted by subscripts d and r, respectively. The complex amplitudes of the diffracted/radiated waves are here expressed in terms of θ-dependent complex functions $H_{\mathrm{d/r}}(\theta)$, the so-called Kochin functions, whose relation to the outgoing waves' velocity potential is given by equation (A 5). It should be noted that the mathematical connection of the, explicit, leading term in equation (A 3) with the definition (A 5) is far from trivial. Details, which include, for example, integral evaluation by the stationary-phase method, are omitted here, but explained through several mathematical steps by, for example, Falnes [43, p. 101]. Adopting notation as in §§4.7 and 4.8 of the same cited reference, the velocity potentials corresponding to wave elevations η, η_0, η_d and η_r have complex amplitudes as given by the line vector

$$(\hat{\phi}\ \Phi\ \psi_\mathrm{d}\ \psi_\mathrm{r}) = \left(\frac{\mathrm{i}g}{\omega}\right)\mathrm{e}(kz)(\hat{\eta}\ \hat{\eta}_0\ \hat{\eta}_\mathrm{d}\ \hat{\eta}_\mathrm{r}), \tag{A 4}$$

where $\mathrm{e}(kz) = \cosh(kz + kh)/\cosh(kh)$, which we, for the deep-water case $(kh \gg 1)$, may replace by e^{kz}. (The z-axis is pointing upwards, and the plane $z = 0$ coincides with the mean water level.) The velocity potentials $\psi_j = \psi_j(r, \theta, z)$ $(j = \mathrm{d}, \mathrm{r})$ satisfy the radiation condition of outgoing waves at infinity, that is, as $kr \to \infty$. It will here be convenient to introduce the phase velocity

$v_\mathrm{p} = \omega/k = (g/\omega)\tanh(kh)$ and the group velocity $v_\mathrm{g} = (g/\omega)D(kh)/2$, where $D(kh) = 2k\int_{-h}^{0}[\cosh(kz+kh)/\cosh(kh)]^2\,\mathrm{d}z = \tanh(kh) + kh - kh\tanh^2(kh)$. The Kochin functions $H_\mathrm{d/r}(\theta)$ for the outgoing diffracted/radiated waves are related to their velocity potentials $\psi_\mathrm{d/r}$ through [35, eqns (16)–(18)]

$$H_\mathrm{d/r}(\beta) = -\frac{g}{2v_\mathrm{p}v_\mathrm{g}}\mathcal{I}\left(\left(\frac{\mathrm{i}g}{\omega}\right)\mathrm{e}(kz)\,\mathrm{e}^{\mathrm{i}kr\cos(\theta-\beta)}, \psi_\mathrm{d/r}\right), \tag{A 5}$$

where the very useful integral

$$\mathcal{I}(\phi_i,\phi_j) \equiv \int\!\!\int_S \left(\phi_i\frac{\partial\phi_j}{\partial n} - \frac{\partial\phi_i}{\partial n}\phi_j\right)\mathrm{d}S = \int_0^{2\pi}\int_{-h}^{0}\left(\phi_i\frac{\partial\phi_j}{\partial r} - \frac{\partial\phi_i}{\partial r}\phi_j\right) r\,\mathrm{d}\theta\,\mathrm{d}z \tag{A 6}$$

has been introduced. The surface of integration S is the totality of all energy-exchanging (wave-generating or wave-absorbing) surfaces, i.e. wet surfaces S_i of immersed oscillating bodies and oscillating air–water interfaces S_k of OWCs (figure 5). Further, $\partial/\partial n$ denotes the into-the-fluid-pointing normal component of the gradient. Moreover, ϕ_i and ϕ_j are two arbitrary functions (e.g. velocity potentials) that satisfy, firstly, the Laplace equation everywhere in the fluid region and, secondly, also all homogeneous boundary conditions that any velocity potential should satisfy on that part of the fluid-containing closed boundary which is complementary to the energy-exchanging surface, S. Note that it follows from the definition (A 6) that $\mathcal{I}(\phi_j,\phi_i) = -\mathcal{I}(\phi_i,\phi_j)$. The usefulness of the integral is that, because of Green's theorem, the integration surface may be moved further into the fluid without changing the value of the integral, as exemplified by the r.h.s. of equation (A 6), where the surface of integration is cylindrical and has a radius r that may tend to infinity. See the envisaged cylindrical control surface S_∞ in figure 5. For mathematical convenience, a constant water depth h is assumed outside, but not necessarily inside, S_∞. As we shall discuss in the following, some of the general results given by Newman [35] are applicable for the more general case as indicated in figure 5, even though Newman considered the single-body case only.

Because of the implied ideal-fluid assumption, there is no energy loss associated with wave propagation. Hence, the wave power P_a that is absorbed by the group of immersed WEC units, provided they are oscillating and consequently radiating, must be equal to the wave power that is transported from the outside to the inside of the envisaged vertical cylindrical surface S_∞ of radius r, even if $r\to\infty$. Thus

$$P_\mathrm{a} = -\int_0^{2\pi} J_r(r,\theta)r\,\mathrm{d}\theta = -\int_0^{2\pi}\int_{-h}^{0}\frac{1}{2}\,\Re\{\hat{p}\hat{v}_\mathrm{r}^*\}r\,\mathrm{d}\theta\,\mathrm{d}z, \tag{A 7}$$

where J_r is the r component of the wave power-level vector J. Further, $\hat{p} = \hat{p}(r,\theta,z) = -\mathrm{i}\omega\rho\hat{\phi} = \rho g\hat{\eta}\cosh(kz+kh)/\cosh(kh)$ and $\hat{v}_\mathrm{r} = \hat{v}_\mathrm{r}(r,\theta,z) = (\partial/\partial r)\hat{\phi}(r,\theta,z)$ are the complex amplitudes of the hydrodynamic pressure and of the fluid velocity's r component, respectively. Moreover, ρ is the mass density of water, and the asterisk (*) denotes complex conjugate. By inserting for $\hat{p}$ and $\hat{v}_\mathrm{r}$ into equation (A 7), we may write the absorbed wave power as [35, eqn (58)]

$$P_\mathrm{a} = \frac{\mathrm{i}\omega\rho}{4}\,\mathcal{I}(\hat{\phi},\hat{\phi}^*) = \frac{\mathrm{i}\omega\rho}{4}\,\mathcal{I}(\Phi+\psi_\mathrm{d}+\psi_\mathrm{r}, \Phi^*+\psi_\mathrm{d}^*+\psi_\mathrm{r}^*). \tag{A 8}$$

We may note that $\mathcal{I}(\Phi, \Phi^*) = 0$, that is, no net energy is flowing through the cylindrical control surface S_∞ if there is no other wave than the undisturbed incident plane wave, as would have been the case if the water depth had been constant, and equal to h, also everywhere inside this surface, and if, in addition, all energy-exchanging objects had been removed. In this case, there is no diffracted wave and no radiated wave. In the general case, we discriminate between diffracted and radiated waves by imposing the condition that the r.h.s. of equation (A 8) vanishes when $\psi_\mathrm{r} \equiv 0$, that is when no power can be absorbed. Hence

$$\mathcal{I}(\Phi + \psi_\mathrm{d}, \Phi^* + \psi_\mathrm{d}^*) = 0. \tag{A 9}$$

Thus, equation (A 8) is reduced to

$$P_\mathrm{a} = \frac{\mathrm{i}\omega\rho}{4}[\mathcal{I}(\Phi + \psi_\mathrm{d}, \psi_\mathrm{r}^*) - \mathcal{I}(\Phi^* + \psi_\mathrm{d}^*, \psi_\mathrm{r}) + \mathcal{I}(\psi_\mathrm{r}, \psi_\mathrm{r}^*)]. \tag{A 10}$$

This may be written as

$$P_\mathrm{a} = P_\mathrm{e} - P_\mathrm{r} = (AE^* + A^*E) - |D|^2 = \left|\frac{AE}{D}\right|^2 - \left|\frac{AE^*}{D^*} - D\right|^2, \tag{A 11}$$

where $P_\mathrm{e} = AE^* + A^*E$ is the excitation power and

$$P_\mathrm{r} = |D|^2 = -\frac{\mathrm{i}\omega\rho}{4}\mathcal{I}(\psi_\mathrm{r}, \psi_\mathrm{r}^*) = \frac{\omega\rho v_\mathrm{p} v_\mathrm{g}}{4\pi g}\int_0^{2\pi} |H_\mathrm{r}(\theta)|^2 \,\mathrm{d}\theta \tag{A 12}$$

is the (non-negative) radiated power. Moreover,

$$E = -\frac{\mathrm{i}\omega\rho}{4A^*}\mathcal{I}(\Phi^* + \psi_\mathrm{d}^*, \psi_\mathrm{r}) = \frac{\rho v_\mathrm{p} v_\mathrm{g}}{2}\left(H_\mathrm{r}(\beta) - \frac{\omega}{2\pi g}\int_0^{2\pi} \frac{H_\mathrm{d}^*(\theta)}{A^*} H_\mathrm{r}(\theta)\,\mathrm{d}\theta\right). \tag{A 13}$$

When deriving the r.h.s. of equation (A 12) and the last term of equation (A 13), we made use of equations (A 3), (A 4) and (A 6). Moreover, we applied equations (A 2), (A 4) and (A 5) to derive the term with $H_\mathrm{r}(\beta)$ in equation (A 13).

Observe that, since Φ/A, ψ_d/A and $H_\mathrm{d}(\theta)/A$ are independent of the complex amplitude A of the incident wave, the complex-valued E, which is a function of the angle of wave incidence β, is linearly related to the radiated wave. We have not, so far, considered local details at the wave energy-interacting objects indicated in figure 5. Thus, the above derivation is a global analysis. Global results, analogous to equations (A 11)–(A 13), were derived by Newman [35, eqn (61b)], for the WEC case of only one single immersed body, and by Budal [47, eqn (26)], for the case of a group of several immersed bodies. In our present case, the group of WEC units may also contain OWCs.

By inspection, we see from the r.h.s. of equation (A 11) that the maximum absorbed power is $P_\mathrm{a,MAX} = |AE/D|^2$, which is obtained for the optimum condition $AE^*/D^* - D = 0$, or $AE^* = |D|^2 = A^*E$. Consequently, for the radiated wave, there exists an optimum Kochin function $H_{\mathrm{r},0}(\theta)$, which has to satisfy the

following integral equation:

$$A^* H_{\mathrm{r},0}(\beta) = \frac{\omega}{2\pi g} \int_0^{2\pi} [H_{\mathrm{d}}^*(\theta) + H_{\mathrm{r},0}^*(\theta)] H_{\mathrm{r},0}(\theta)\, \mathrm{d}\theta. \tag{A 14}$$

We denote the corresponding optimum values of D and E as D_0 and E_0. Moreover, we denote as $\psi_{\mathrm{r},0}$ the velocity potential for any radiated wave that has a Kochin function satisfying equation (A 14). Note, however, that the near-field part of this wave may be ambiguous. From the above discussion of the optimum case, it follows that we have several different alternative expressions for the maximum absorbed power, e.g.

$$P_{\mathrm{a,MAX}} = P_{\mathrm{r,OPT}} = |D_0|^2 = \frac{P_{\mathrm{e,OPT}}}{2} = AE_0^* = A^* E_0 = |AE_0|. \tag{A 15}$$

Moreover, we shall find it convenient to write it as

$$P_{\mathrm{a,MAX}} = \frac{(P_{\mathrm{a,MAX}})^2}{P_{\mathrm{a,MAX}}} = \frac{(P_{\mathrm{e,OPT}}/2)^2}{P_{\mathrm{r,OPT}}} = \frac{(AE_0^*)^2}{|D_0|^2} = \frac{(A^* E_0)^2}{|D_0|^2} = \frac{|AE_0|^2}{|D_0|^2}. \tag{A 16}$$

Applying the penultimate one of the fractions shown in equations (A 16), and then inserting from equations (A 12) and (A 13), we get

$$P_{\mathrm{a,MAX}} = \frac{(A^* E_0)^2}{|D_0|^2} = \frac{\rho g v_{\mathrm{g}} |A|^2}{2k} G(\beta) = \left(\frac{J}{k}\right) G(\beta) = J d_{\mathrm{a,MAX}}, \tag{A 17}$$

where $J = \rho g v_{\mathrm{g}} |A|^2/2$ is the incident wave-power level, and $d_{\mathrm{a}} \equiv P_{\mathrm{a}}/J$ is the 'absorption width'. Moreover, we have introduced the gain function

$$G(\beta) = \frac{2\pi |H_{\mathrm{r},0}(\beta) - (\omega/2\pi g) \int_0^{2\pi} (H_{\mathrm{d}}(\theta)/A)^* H_{\mathrm{r},0}(\theta)\, \mathrm{d}\theta|^2}{\int_0^{2\pi} |H_{\mathrm{r},0}(\theta)|^2\, \mathrm{d}\theta}. \tag{A 18}$$

So far, the above analysis is global. Results have been obtained by considering wave interference in the far-field region. By considering physical parameters and boundary conditions at the wave-interacting WEC units, we may eliminate the integral in the numerator of equation (A 18), and thus obtain an expression for $G(\beta)$ not explicitly dependent on the Kochin function $H_{\mathrm{d}}(\theta)$ for the diffracted wave. A clue to this elimination is the Haskind relation, by which the excitation force, even though it is a diffraction parameter, may be expressed in terms of a radiation parameter.

It was shown by Newman [42, eqn (9)] and also by Evans [36,57, eqn (2.10)] that the numerator in the fraction of equation (A 18) may be simplified to $2\pi |H_{\mathrm{r},0}(\beta + \pi)|^2$ for the simple case of only one single immersed body when only one of the six possible modes of oscillation, mode j, say, is used. The wave-excitation force has a complex amplitude $\hat{F}_{\mathrm{e},j}(\beta) = f_j(\beta) A$. For this case, the maximum absorbed power, as given by the last three of equations (A 15), is

$$P_{\mathrm{a,MAX}} = \frac{A f_j(\beta) \hat{u}_{j,0}^*}{4} = \frac{A^* f_j^*(\beta) \hat{u}_{j,0}}{4} = \frac{|A f_j(\beta) \hat{u}_{j,0}|}{4},$$

which because of the Haskind relation is proportional to

$$A h_j(\beta + \pi) \hat{u}_{j,0}^* = A^* h_j^*(\beta + \pi) \hat{u}_{j,0} = |A h_j(\beta + \pi) \hat{u}_{j,0}| = |A H_{\mathrm{r},0}(\beta + \pi)|.$$

We may note that the quantity $\bar{H}_{\mathrm{r},0}(\beta+\pi)=h_j(\beta+\pi)\hat{u}^*_{j,0}$, which is the Kochin function if the complex velocity amplitude is $\hat{u}^*_{j,0}$ instead of $\hat{u}_{j,0}$, may, for the one-mode case, differ from $H_{\mathrm{r},0}(\beta+\pi)=h_j(\beta+\pi)\hat{u}_{j,0}$ in phase, but not in magnitude. Note that complex conjugation in the frequency plane corresponds to time-reversal in the time domain. (But, for a single-mode single-body case, $\bar{H}_{\mathrm{r},0}(\beta+\pi)$ equals, however, $H_{\mathrm{r},0}(\beta+\pi)$ if A is real and positive.)

Next, let us consider a single body that oscillates in two modes, surge ($j=1$) and heave ($j=3$), with complex velocity amplitudes $\hat{u}_j$. The resulting body motion may be represented by the complex amplitude velocity vector $\hat{\mathbf{u}}\equiv[\hat{u}_1\ \hat{u}_3]^{\mathrm{T}}$, where the superscript T symbol denotes transpose. The body motion may then be considered as an elliptically polarized oscillation in the xz plane. The body is orbiting in a clockwise direction if $0<(\angle\hat{u}_3-\angle\hat{u}_1)<\pi$, that is, if surge lags in phase behind heave. Observe that oscillations represented by $\hat{\mathbf{u}}$ and $\hat{\mathbf{u}}^*=[\hat{u}^*_1\ \hat{u}^*_3]^{\mathrm{T}}$ orbit in opposite directions. If, for instance, $\hat{u}_1=\pm\mathrm{i}\hat{u}_3$, then the elliptic orbit specializes to a circular orbit.

If the body has an optimum motion, that is, if $\hat{\mathbf{u}}=\hat{\mathbf{u}}_0=[\hat{u}_{1,0}\ \hat{u}_{3,0}]^{\mathrm{T}}$, then the maximum absorbed power may be written as (cf. Falnes [43], pp. 158–159, 215)

$$P_{\mathrm{a,MAX}}=\frac{P_{\mathrm{e,OPT}}}{2}=\frac{\hat{\mathbf{F}}_{\mathrm{e}}^{\mathrm{T}}\hat{\mathbf{u}}_0^*}{4}=\frac{\hat{\mathbf{u}}_0^{\mathrm{T}}\hat{\mathbf{F}}_{\mathrm{e}}^*}{4}, \tag{A 19}$$

where the complex amplitude vector for the excitation forces is given by

$$\begin{aligned}\hat{\mathbf{F}}_{\mathbf{e}}=\hat{\mathbf{F}}_{\mathbf{e}}(\beta)&=[\hat{F}_{\mathrm{e},1}(\beta)\ \hat{F}_{\mathrm{e},3}(\beta)]^{\mathrm{T}}=[f_1(\beta)\ f_3(\beta)]^{\mathrm{T}}A\\&=2\rho v_{\mathrm{g}}v_{\mathrm{p}}[h_1(\beta+\pi)\ h_3(\beta+\pi)]^{\mathrm{T}}A\equiv 2\rho v_{\mathrm{g}}v_{\mathrm{p}}\mathbf{h}(\beta+\pi)A,\end{aligned} \tag{A 20}$$

where $f_j(\beta)$ is an excitation-force coefficient and $h_j(\theta)$ a Kochin-function coefficient. Note that we have here applied the Haskind relation between $f_j(\beta)$ and $h_j(\beta+\pi)$. The optimum Kochin function for the radiated wave is

$$H_{\mathrm{r},0}(\theta)=h_1(\theta)\hat{u}_{1,0}+h_3(\theta)\hat{u}_{3,0}=\mathbf{h}^{\mathrm{T}}(\theta)\hat{\mathbf{u}}_0, \tag{A 21}$$

when the WEC oscillation state is given by the optimum velocity vector $\hat{\mathbf{u}}_0$, and by

$$\mathbf{h}^{\mathrm{T}}(\theta)\hat{\mathbf{u}}_0^*\equiv\bar{H}_{\mathrm{r},0}(\theta) \tag{A 22}$$

with $\hat{\mathbf{u}}_0^*$ instead of $\hat{\mathbf{u}}_0$. Note that the motion of the body oscillating in surge and heave is an elliptically polarized oscillation, where the two cases $\hat{\mathbf{u}}_0^*$ and $\hat{\mathbf{u}}_0$ correspond to opposite directions of motion along the elliptical orbit. With optimum velocity vector $\hat{\mathbf{u}}_0$, the maximum absorbed power is $P_{\mathrm{a,MAX}}=P_{\mathrm{e,OPT}}/2$, where

$$P_{\mathrm{e,OPT}}=\frac{\hat{\mathbf{F}}_{\mathrm{e}}^{\mathrm{T}}\hat{\mathbf{u}}_0^*}{2}=\rho v_{\mathrm{g}}v_{\mathrm{p}}\mathbf{h}^{\mathrm{T}}(\beta+\pi)A\hat{\mathbf{u}}_0^*=\rho v_{\mathrm{g}}v_{\mathrm{p}}\bar{H}_{\mathrm{r},0}(\beta+\pi)A, \tag{A 23}$$

according to equations (A 19), (A 20) and (A 22). If we now compare this equation (A 23) with equations (A 13) and (A 15), we observe that we may replace

the numerator in equation (A 18) by $2\pi|\bar{H}_{\mathrm{r},0}(\beta+\pi)|^2$. Hence, we have simplified this equation to

$$G(\beta)=\frac{2\pi|\bar{H}_{\mathrm{r},0}(\beta+\pi)|^2}{\int_0^{2\pi}|H_{\mathrm{r},0}(\theta)|^2\,\mathrm{d}\theta}. \tag{A 24}$$

In contrast to equation (A 18), the Kochin function $H_{\mathrm{d}}(\theta)$ for the diffracted wave does not enter explicitly into equation (A 24).

For a WEC system that consists of N immersed bodies that oscillate in each of their six modes of motion, the column vectors $\hat{\mathbf{u}}$, $\hat{\mathbf{u}}_0$, $\hat{\mathbf{F}}_{\mathrm{e}}$ and $\mathbf{h}$, which are introduced as two-dimensional vectors in the previous paragraph, may (e.g. Falnes [43, pp. 150, 158, 215]) be generalized to $6N$-dimensional column vectors. Thus, equation (A 24) is applicable even for this, more general, case.

For a WEC system that consists of both oscillating bodies and OWCs (cf. figure 5), the optimum radiation Kochin function to apply in equation (A 18) is

$$H_{\mathrm{r},0}(\theta)=[\mathbf{h}_{\mathbf{u}}^{\mathrm{T}}(\theta)\ \mathbf{h}_{\mathbf{p}}^{\mathrm{T}}(\theta)]\begin{bmatrix}\hat{\mathbf{u}}_0\\ \hat{\mathbf{p}}_0\end{bmatrix}=\mathbf{h}_{\mathbf{u}}^{\mathrm{T}}(\theta)\hat{\mathbf{u}}_0+\mathbf{h}_{\mathbf{p}}^{\mathrm{T}}(\theta)\hat{\mathbf{p}}_0, \tag{A 25}$$

where $\hat{\mathbf{u}}_0$ and $\hat{\mathbf{p}}_0$ are optimum values of the column vectors $\hat{\mathbf{u}}$ and $\hat{\mathbf{p}}$, which represent the complex velocity amplitudes for the oscillating-body WEC units and the complex air-pressure amplitudes for the OWC WEC units, respectively. Note that on the ultimate r.h.s. of equation (A 25), the first term corresponds to the ultimate r.h.s. of equation (A 21). Thus, the column vector $\mathbf{h}_{\mathbf{u}}(\theta)$ is composed of all oscillating-body modes Kochin-function proportionality coefficients, while the column vector $\mathbf{h}_{\mathbf{p}}(\theta)$ collects all OWC-related Kochin-function proportionality coefficients. At optimum, the maximum absorbed power is $P_{\mathrm{a,MAX}}=P_{\mathrm{e,OPT}}/2$, where (cf. Falnes & McIver [38, eqns (27), (29), (67), (68)])

$$P_{\mathrm{e,OPT}}=\frac{1}{2}[\hat{\mathbf{F}}_{\mathrm{e}}^{\mathrm{T}}\ \pm\hat{\mathbf{Q}}_{\mathrm{e}}^{\mathrm{T}}]\begin{bmatrix}\hat{\mathbf{u}}_0^*\\ \pm\hat{\mathbf{p}}_0^*\end{bmatrix}=\frac{\hat{\mathbf{F}}_{\mathrm{e}}^{\mathrm{T}}\hat{\mathbf{u}}_0^*+\hat{\mathbf{Q}}_{\mathrm{e}}^{\mathrm{T}}\hat{\mathbf{p}}_0^*}{2}, \tag{A 26}$$

where the column vectors $\hat{\mathbf{F}}_{\mathrm{e}}$ and $\hat{\mathbf{Q}}_{\mathrm{e}}$ represent the excitation forces and excitation volume flows for the oscillating bodies and OWCs, respectively. According to the Haskind relation, they may be expressed in terms of Kochin-function coefficient vectors, $\mathbf{h}_{\mathbf{u}}$ and $\mathbf{h}_{\mathbf{p}}$, as

$$\begin{bmatrix}\hat{\mathbf{F}}_{\mathrm{e}}\\ \pm\hat{\mathbf{Q}}_{\mathrm{e}}\end{bmatrix}=\begin{bmatrix}\hat{\mathbf{F}}_{\mathrm{e}}(\beta)\\ \pm\hat{\mathbf{Q}}_{\mathrm{e}}(\beta)\end{bmatrix}=2\rho v_{\mathrm{g}}v_{\mathrm{p}}\begin{bmatrix}\mathbf{h}_{\mathbf{u}}(\beta+\pi)\\ \mp\mathbf{h}_{\mathbf{p}}(\beta+\pi)\end{bmatrix}A. \tag{A 27}$$

Note that we may, at our own convenience, choose the upper or the lower sign in equations (A 26) and (A 27); the upper sign was chosen by Falnes & McIver [38]. We now define the adjoint Kochin function

$$\bar{H}_{\mathrm{r},0}(\theta)=[\mathbf{h}_{\mathbf{u}}^{\mathrm{T}}(\theta)\ \mathbf{h}_{\mathbf{p}}^{\mathrm{T}}(\theta)]\begin{bmatrix}\hat{\mathbf{u}}_0^*\\ -\hat{\mathbf{p}}_0^*\end{bmatrix}=\mathbf{h}_{\mathbf{u}}^{\mathrm{T}}(\theta)\hat{\mathbf{u}}_0^*-\mathbf{h}_{\mathbf{p}}^{\mathrm{T}}(\theta)\hat{\mathbf{p}}_0^*, \tag{A 28}$$

and insert equation (A 27) into equation (A 26), which gives

$$P_{\mathrm{e,OPT}}=\rho v_{\mathrm{g}}v_{\mathrm{p}}\bar{H}_{\mathrm{r},0}(\beta+\pi)A. \tag{A 29}$$

If we compare this with equation (A 15) and observe equation (A 13), we find that we may simplify the numerator in equation (A 18) to the one in equation (A 24). We observe that the adjoint Kochin function $\bar{H}_{\mathrm{r},0}(\theta)$ is the Kochin function for a radiated wave in the case where the optimum wave-absorbing oscillation, represented by $\hat{\mathbf{u}}_0$ and $\hat{\mathbf{p}}_0$, is replaced by an oscillation state corresponding to $\hat{\mathbf{u}}_0^*$ and $-\hat{\mathbf{p}}_0^*$, respectively. The opposite sign for the last term in equation (A 28) is related to the fact that the boundary conditions at the air–water interface of QWCs are different from the boundary conditions at the wet surfaces of immersed bodies.

References

1 Masuda, Y. 1972 Study of wave activated generator and future view as an island power source. In *Proc. 2nd Int. Ocean Development Conf., Tokyo, Japan, 4–9 October 1972*, vol. 2, pp. 2074–2090.

2 Masuda, Y. 1986 An experience of wave power generator through tests and improvement. In *Hydrodynamics of ocean wave-energy utilization* (eds D. V. Evans & A. F. d. O. Falcao), pp. 445–452. Berlin, Germany: Springer.

3 McCormick, M. E. 1974 Analysis of a wave energy conversion buoy. *J. Hydronautics* **8**, 77–82. (doi:10.2514/3.62983)

4 Budal, K. & Falnes, J. 1975 A resonant point absorber of ocean-wave power. *Nature* **256**, 478–479. [Corrigendum in *Nature* 1975 **257**, 626.] (doi:10.1038/256478a0)

5 Isaacs, J. D., Castel, D. & Wick, G. L. 1976 Utilization of the energy in ocean waves. *Ocean Eng.* **3**, 175–187. (doi:10.1016/0029-8018(76)90022-6)

6 Bergdahl, L., Claeson, L., Falkemo, C., Forsberg, J. & Rylander, A. 1979 The Swedish wave energy research programme. In *Proc. 1st Symp. on Wave Energy Utilization*, 30 October–1 November 1979, pp. 222–252. Gothenburg, Sweden: Chalmers University of Technology.

7 Evans, D. V. 1981 Power from water waves. *Annu. Rev. Fluid Mech.* **13**, 157–187. (doi:10.1146/annurev.fl.13.010181.001105)

8 Falnes, J. 2002 Optimum control of oscillation of wave-energy converters. *Int. J. Offshore Polar Eng.* **12**, 147–155. (doi:10.1017/CBO9780511754630)

9 Salter, S. H., Jeffery, D. C. & Taylor, J. R. M. 1976 The architecture of nodding duck wave power generators. *Naval Archit.* January, pp. 21–24.

10 Budal, K. & Falnes, J. 1977 Optimum operation of improved wave-power converter. *Mar. Sci. Commun.* **3**, 133–150.

11 Budal, K. & Falnes, J. 1978 *A system for the conversion of sea wave energy*. British Patent no. 1522661.

12 Budal, K. & Falnes, J. 1980 Interacting point absorbers with controlled motion. In *Power from sea waves* (ed. B. Count), pp. 381–399. London, UK: Academic Press.

13 Salter, S. H. 1979 Power conversion systems for ducks. In *Proc. Int. Conf. on Future Energy Concepts, London, UK, 30 January–1 February 1979*, pp. 100–108. Institution of Electrical Engineers, Publication 171.

14 Salter, S. 1980 *Apparatus for extracting power from waves on water*. British Patent no. 1571790.

15 Falnes, J. & Budal, K. 1978 Wave-power conversion by point absorbers. *Norweg. Maritime Res.* **6**, 2–11.

16 Guenther, D., Jones, D. & Brown, D. 1979 An investigative study of a wave-energy device. *Energy* **4**, 299–306. (doi:10.1016/0360-5442(79)90129-4)

17 French, M. 1979 A generalized view of resonant energy transfer. *J. Mech. Eng. Sci.* **21**, 299–300. (doi:10.1243/JMES_JOUR_1979_021_047_02)

18 Greenhow, M., Rosen, J. H. & Reed, M. 1984 Control strategies for the clam wave energy device. *Appl. Ocean Res.* **6**, 197–206. (doi:10.1016/0141-1187(84)90058-0)

19 Salter, S. H., Taylor, J. R. M. & Caldwell, N. J. 2002 Power conversion mechanisms for wave energy. *Proc. Inst. Mech. Eng. M* **216**, 1–27. (doi:10.1243/147509002320382103)

20 Babarit, A., Mouslim, H., Guglielmi, M. & Clément, A. H. 2008 Simulation of the SEAREV wave energy converter with a by-pass control of its hydraulic power take off. In *Proc. 10th World Renewable Energy Congress* (*WRECX*), *Glasgow, UK, 19–25 July 2008*, pp. 1004–1009.
21 Babarit, A., Guglielmi, M. & Clément, A. H. 2009 Declutching control of a wave energy converter. *Ocean Eng.* **36**, 1015–1024. (doi:10.1016/j.oceaneng.2009.05.006)
22 Gieske, P. 2007 Model predictive control of a wave energy converter: Archimedes wave swing. Master's thesis, Delft University of Technology, The Netherlands.
23 Hals, J., Falnes, J. & Moan, T. 2011 Constrained optimal control of a heaving buoy wave-energy converter. *J. Offshore Mech. Arctic Eng.* **133**, 011401. (doi:10.1115/1.4001431)
24 Bacelli, G., Gilloteaux, J.-C. & Ringwood, J. 2009 A predictive controller for a heaving buoy producing potable water. In *Proc. European Control Conf., Budapest, Hungary, 23–26 August 2009*.
25 Cretel, J., Lewis, A. W., Lightbody, G. & Thomas, G. P. 2010 An application of model predictive control to a wave energy point absorber. In *IFAC Conf. on Control Methodologies and Technology for Energy Efficiency, Vilamoura, Portugal, 29–31 March 2010*.
26 Budal, K., Falnes, J., Hals, T., Iversen, L. C. & Onshus, T. 1981 Model experiment with a phase controlled point absorber. In *Proc. 2nd Int. Symp. on Wave and Tidal Energy* (eds H. S. Stephens & C. A. Stapleton), pp. 191–206. Cambridge, UK: BHRA.
27 Fusco, F. & Ringwood, J. 2009 A study on short-term sea profile prediction for wave energy applications. In *Proc. 8th European Wave and Tidal Energy Conf., Uppsala, Sweden, 7–10 September 2009*.
28 Budal, K. 1978 Kraftbøye: System E. Internal memo, Institutt for eksperimentalfysikk, NTH, Trondheim. [Reissued as Annex A in 'Preliminary design and model test of a wave-power converter: Budal's 1978 design Type E', compiled by J. Falnes. Institutt for fysikk, NTH, 1993.]
29 Falnes, J. & Lillebekken, P. M. 2003 Budal's latching-controlled-buoy type wave-power plant. In *Proc. 5th European Wave Energy Conf.* (eds A. Lewis & G. Thomas), pp. 233–244. Cork, Ireland: Hydraulics and Maritime Research Centre (HMRC).
30 Falnes, J. & Lillebekken, P. M. 2007 Wave-energy research at NTH/NTNU. See http://folk.ntnu.no/falnes/w_e/index-e.html.
31 Naito, S. & Nakamura, S. 1986 Wave energy absorption in irregular waves by feed forward control system. In *Hydrodynamics of ocean wave-energy utilization* (eds D. V. Evans & A. F. d. O. Falcao), pp. 269–280. Berlin, Germany: Springer.
32 Perdigão, J. N. B. A. & Sarmento, A. J. N. A. 1989 A phase control strategy for OWC devices in irregular seas. In *Proc. 4th Int. Workshop on Water Waves and Floating Bodies* (ed. J. Grue), pp. 205–209. Oslo, Norway: Department of Mathematics, University of Oslo.
33 Budal, K., Falnes, J., Kyllingstad, A. & Oltedal, G. 1979 Experiments with point absorbers. In *Proc. 1st Symp. on Wave Energy Utilization*, 30 October–1 November 1979, pp. 253–282. Gothenburg, Sweden: Chalmers University of Technology.
34 Keulegan, G. H. & Carpenter, L. H. 1958 Forces on cylinders and plates in an oscillating fluid. *J. Res. Natl Bureau Standards* **60**, 423–440.
35 Newman, J. N. 1976 The interaction of stationary vessels with regular waves. In *Proc. 11th Symp. on Naval Hydrodynamics, London, UK, 28 March–2 April 1976*, pp. 491–501.
36 Evans, D. V. 1980 Some analytic results for two and three dimensional wave-energy absorbers. In *Power from sea waves* (ed. B. Count), pp. 213–249. New York, NY: Academic Press.
37 Falnes, J. 1980 Radiation impedance matrix and optimum power absorption for interacting oscillators in surface waves. *Appl. Ocean Res.* **2**, 75–80. (doi:10.1016/0141-1187(80)90032-2)
38 Falnes, J. & McIver, P. 1985 Surface wave interactions with systems of oscillating bodies and pressure distributions. *Appl. Ocean Res.* **7**, 225–234. (doi:10.1016/0141-1187(85)90029-X)
39 Evans, D. V. 1976 A theory for wave-power absorption by oscillating bodies. *J. Fluid Mech.* **77**, 1–25. (doi:10.1017/S0022112076001109)
40 Mei, C. C. 1976 Power extraction from water waves. *J. Ship Res.* **20**, 63–66.
41 Farley, F. J. M. 1982 Wave energy conversion by flexible resonant rafts. *Appl. Ocean Res.* **4**, 57–63. (doi:10.1016/S0141-1187(82)80022-9)

42 Newman, J. N. 1979 Absorption of wave energy by elongated bodies. *Appl. Ocean Res.* **1**, 189–196. (doi:10.1016/0141-1187(79)90026-9)
43 Falnes, J. 2002 *Ocean waves and oscillating systems: linear interactions including wave-energy extraction*. Cambridge, UK: Cambridge University Press.
44 Evans, D. V. 1988 The maximum efficiency of wave-energy devices near coast lines. *Appl. Ocean Res.* **10**, 162–164. (doi:10.1016/S0141-1187(88)80016-6)
45 Shaw, R. 1982 *Wave energy: a design challenge*. Chichester, UK: Ellis Horwood.
46 Department of Energy. 1979 *Energy paper number 42: wave energy*. London, UK: HMSO.
47 Budal, K. 1977 Theory of absorption of wave power by a system of interacting bodies. *J. Ship Res.* **21**, 248–253.
48 Grove-Palmer, C. O. J. 1982 Wave energy in the United Kingdom. A review of the programme June 1975–March 1982. In *Proc. 2nd Int. Symp. on Wave Energy Utilization. 22–24 June 1982*, (ed. H. Berge), pp. 23–54. Trondheim, Norway: Tapir.
49 Count, B. M. 1980 Wave power: a problem searching for a solution. In *Power from sea waves* (ed. B. Count), pp. 11–27. London, UK: Academic Press.
50 Pizer, D. 1993 Maximum wave-power absorption of point-absorbers under motion constraints. *Appl. Ocean Res.* **15**, 227–234. (doi:10.1016/0141-1187(93)90011-L)
51 McCabe, A. P. & Aggidis, G. A. 2009 Optimum mean power output of a point-absorber wave energy converter in irregular waves. *Proc. Inst. Mech. Eng. A* **223**, 773–781. (doi:10.1243/09576509JPE751)
52 Hals, J. Submitted. Practical limits to the power that can be captured from ocean waves by oscillating bodies.
53 Rademakers, L. W. M. M., van Schie, R. G., Schuitema, R., Vriesema, B. & Gardner, F. 2000 Physical model testing for characterising the AWS wave power generating plant. In *Proc. 3rd European Int. Wave Power Conf., Patras, Greece, 30 September–2 October 1998* (ed. W. Dursthoff), pp. 192–199. Hannover, Germany: University of Hannover.
54 Garnaud, X. & Mei, C. C. 2009 Comparison of wave power extraction by a compact array of small buoys and by a large buoy. In *Proc. 8th European Wave and Tidal Energy Conf., Uppsala, Sweden, 7–10 September 2009*, pp. 934–942.
55 Falnes, J. 1994 Small is beautiful: how to make wave energy economic. In *Proc. Int. Symp. on European Wave Energy, Edinburgh, UK, 21–24 July 1993* (eds G. Elliot & G. Caratti), pp. 367–372. East Kilbride, UK: National Engineering Laboratory Executive Agency.
56 Ambli, N., Budal, K., Falnes, J. & Sørenssen, A. 1977 Wave power conversion by a row of optimally operated buoys. In *Proc. 10th World Energy Conf. Istanbul, Turkey, 19–23 September 1977*, vol. 4, paper 4.5-2.
57 Evans, D. V. 1979 Some theoretical aspects of three-dimensional wave-energy absorbers. In *Proc. 1st Symp. on Wave Energy Utilization*, 30 October–1 November 1979, pp. 77–113. Gothenburg, Sweden: Chalmers University of Technology.